Antiviral Research 230 (2024) 105990

Contents lists available at ScienceDirect

Antiviral Research

journal homepage: www.elsevier.com/locate/antiviral

Discovery of a small-molecule inhibitor of KSHV lytic replication from the MMV pandemic response box

Michael O. Okpara [a], Frederick Weaver [b], Adrian Whitehouse [a,b,c,d], Clinton G.L. Veale [e], Adrienne L. Edkins [a,f,*]

[a] Biomedical Biotechnology Research Unit (BioBRU), Department of Biochemistry and Microbiology, Rhodes University, Grahamstown, South Africa
[b] School of Molecular and Cellular Biology, Faculty of Biological Sciences, University of Leeds, Leeds, LS2 9JT, UK
[c] Astbury Centre for Structural Molecular Biology, University of Leeds, Leeds, LS2 9JT, UK
[d] LeedsOmics, University of Leeds, Leeds, LS2 9JT, UK
[e] Department of Chemistry, University of Cape Town, Rondebosch, Cape Town, South Africa
[f] Centre for Chemico- and Biomedicinal Research (CCBR), Rhodes University, Grahamstown, South Africa

ARTICLE INFO

Keywords:
Kaposi's sarcoma-associated herpesvirus
KSHV
ORF57
Lytic replication
MMV
Pandemic response box
Aminopyrimidone

ABSTRACT

Kaposi's sarcoma-associated herpesvirus (KSHV) is the causative agent for primary effusion lymphoma (PEL), multicentric Castleman's disease (MCD) and Kaposi's sarcoma (KS). KSHV is one of the oncoviruses that contribute to 1.5 million new infection-related cancer cases annually. Currently, there are no targeted therapies for KSHV-associated diseases. Through the development of a medium-throughput phenotype-based ELISA screening platform based on KSHV ORF57 protein detection, we screened the Medicines for Malaria Venture (MMV) Pandemic Response Box for non-cytotoxic inhibitors of KSHV lytic replication. MMV1645152 was identified as a promising inhibitor of KSHV lytic replication, suppressing KSHV immediate-early and late lytic gene expression and blocking the production of infectious KSHV virion particles at non-cytotoxic concentrations in cell line models of KSHV infection with or without EBV coinfection. MMV1645152 is a promising hit compound for the development of future therapeutic agents against KSHV-associated malignancies.

1. Introduction

Kaposi's sarcoma-associated herpesvirus (KSHV) is the causative agent for two lymphoproliferative malignancies, primary effusion lymphoma (PEL) and multicentric Castleman's disease (MCD); and the endothelial malignancy, Kaposi's sarcoma (KS) (Cesarman et al., 2022). KSHV contributes to the incidence of at least 1.5 million new cancer cases by oncoviruses annually (Lunn et al., 2017) and has been classified as a Class 1 carcinogen (Bouvard et al., 2009; Chen et al., 2021). KSHV has a biphasic lifecycle where the virus exists either in a latent phase, allowing the long term persistence of the viral episome where few viral genes are expressed, or reactivates initiating lytic replication, where the majority of the viral genes are expressed resulting in production of infectious virions and ultimately death of the host cell (Aneja and Yuan, 2017).

Upon reactivation, a temporal cascade of expression is triggered leading to the full complement of lytic genes. This occurs in three chronological stages namely the immediate early, delayed early and late lytic phases. Immediate early lytic genes are produced rapidly after reactivation, commencing with the expression of KSHV ORF50 which encodes the replication and transcription activator (RTA). KSHV ORF50/RTA transactivates several KSHV lytic promoters, modulating the switch between KSHV latent and lytic phases. The protein products of immediate early genes initiate the transcription of delayed early genes and subvert host cell processes essential for efficient infectious virion production (Goodwin et al., 2001; Gould et al., 2009; Kirigin et al., 2020).

KSHV ORF57, which encodes the mRNA transcript accumulation (Mta) protein, is an essential immediate early lytic gene which regulates the expression of other lytic genes, promotes viral transcription, and is essential for the production of infectious virion particles (Han and Swaminathan, 2006; Verma et al., 2015). KSHV ORF57 regulates RNA stability and is involved in the export and translation of viral genes (Boyne et al., 2008, 2010; Majerciak and Zheng, 2009). Accordingly,

* Corresponding author. Biomedical Biotechnology Research Unit (BioBRU), Department of Biochemistry and Microbiology, Rhodes University, Grahamstown, South Africa.
E-mail address: a.edkins@ru.ac.za (A.L. Edkins).

https://doi.org/10.1016/j.antiviral.2024.105990
Received 12 January 2024; Received in revised form 2 August 2024; Accepted 14 August 2024
Available online 16 August 2024

KSHV ORF57 plays a critical role in KSHV lytic replication (Purushothaman et al., 2015), making KSHV ORF57 a good marker for the discovery of therapeutic agents blocking early stages of lytic replication.

Despite decades of research on KSHV, there are still no FDA approved vaccines or targeted therapeutic interventions for the treatment of KSHV-associated malignancies. Inhibitors of KSHV lytic replication, including valganciclovir, zidovudine, cidofovir, cyclopropavir, adefovir, acyclovir, and foscarnet sodium which target the viral DNA polymerase (Bounaadja et al., 2013; Coen et al., 2014; Naimo et al., 2021; Ozbalak et al., 2013; Uldrick et al., 2011; Upadhyayula and Michaels, 2013), have been identified as potential therapeutic agents against KSHV. However, poor clinical outcomes, including relapse, and haematological toxicity prevented their clinical approval (Cesarman et al., 2022; Ozbalak et al., 2013; Uldrick et al., 2011, 2012). Chemotherapeutic agents such as vinblastine, cyclophosphamide, and etoposide either alone or in combination, are approved under treatment plans in the US, Europe, and South Africa for KSHV-associated malignancies. But like the inhibitors of lytic replication, they were not without issue (Cesarman et al., 2022). Despite several host-based pathways, such as UAP56, mammalian target of rapamycin (mTOR), EphA2, p38 mitogen-activated protein kinase (MAPK) and topoisomerases I and II, being essential for the KSHV lytic life cycle, inhibition of these targets is either not sufficient to clear KSHV infection in patients or the inhibitors are potential immunosuppressants that reduce the recovery of AIDS-associated KS patients (Andrei and Snoeck, 2015; Mohanty et al., 2017; Nichols et al., 2011; Schumann et al., 2016). On this basis, there remains a need for novel therapeutic agents which specifically target KSHV lytic replication through other mechanisms.

Recently, the Medicine for Malaria Venture (MMV) and the Drugs for Neglected Diseases initiative (DND*i*), launched a library of 400 drug-like compounds called the Pandemic Response Box (which was modelled after the Malaria box and the Pathogen box) (Veale, 2019). The 400 compounds in the Pandemic Response Box include 201 antibacterial compounds, 153 antiviral compounds and 46 antifungal compounds (Samby et al., 2022) and were selected based on low toxicity to mammalian cells and activity against specific microbial pathogens (Medicines for Malaria Venture, 2019).

Here we report the development of a medium-throughput phenotype-based assay to monitor KSHV ORF57 expression and cytotoxicity to host cells as a proxy for inhibition of KSHV lytic replication. A screen of the MMV Pandemic Response Box identified six active compounds, the most promising of which (MMV154152) displayed the best selectivity indices for KSHV lytic replication inhibition.

2. Material and methods

2.1. Cell culture and reagents

The TREx-BCBL-1-RTA cell line (a gift from Prof. Jae Jung, University of Southern California, USA) is a genetically modified derivative of KSHV-infected BCBL-1-based PEL B-cells that contains the RTA gene under the control of a tetracycline-responsive promoter. The induction of KSHV lytic replication was initiated by the addition of 2 μg/mL DOX to TREx-BCBL-1-RTA cells (Nakamura et al., 2003). The BC-1 (CRL-2230™) cell line was purchased from ATCC (Virginia, USA). BC-1 is a Burkitt's lymphoma cell line that is latently infected with KSHV and EBV. In this study, KSHV lytic replication was induced in BC-1 cells by the addition of 1.5 mM sodium butyrate (NaB) (Sandhu and Damania, 2022). HEK293T cells (ATCC®CRL-3216™) were purchased from ATCC. HEK293T is a human embryonic kidney-derived cell line immortalised by transformation with SV40 T-antigen (Graham et al., 1977). The rKSHV.219 cells (a generous gift from Dr Jeffrey Vieira, University of Washington, USA) are HEK293T cells carrying a recombinant form of KSHV genome (KSHV.219) (Vieira and O'Hearn, 2004). KSHV lytic replication in rKSHV.219 cells was induced by the addition of 4 mM NaB and 20 ng/mL 12-*O*-tetradecanoylphorbol-13-acetate (TPA).

TREx-BCBL-1-RTA cells were cultured in Roswell Park Memorial Institute (RPMI) 1640 medium (Thermo Fisher Scientific, USA) supplemented with 10% (v/v) heat-inactivated fetal bovine serum (FBS) (Gibco, UK), 1% (v/v) penicillin-streptomycin-amphotericin (PSA) (Lonza Group Ltd, Basel, Switzerland), 1% (v/v) GlutaMAX™-I (Gibco™, Life Technologies, US) and 100 μg/mL hygromycin B (Glentham Life Sciences, UK). BC-1 cells were cultured in RPMI 1640 medium supplemented with 20% (v/v) FBS, 1% (v/v) PSA, and 1% (v/v) GlutaMAX™-I. TREx-BCBL-1-RTA and BC-1 cell lines were cultured at 37 °C in a humidified incubator with 5% CO_2. HEK293T cells were cultured in Dulbecco's Modified Eagle Medium (DMEM) (LTC Tech, Johannesburg, South Africa) supplemented with 10% (v/v) FBS, 1% (v/v) sodium pyruvate (Sigma-Aldrich, Darmstadt, Germany), 1% (v/v) non-essential amino acids (Lonza, BE13-114E), 1% (v/v) PSA, 1% (w/v) G418 (Glentham Life Sciences, GA2946), and 1% (v/v) GlutaMAX™-I at 37 °C in a humidified incubator with 9% CO_2. The rKSHV.219 cells were cultured in DMEM supplemented with 10% (v/v) FBS, 1% (v/v) PSA, and 2 μg/mL puromycin (Glentham Life Sciences, GA1940) for KSHV genome selection at 37 °C in a humidified incubator with 5% CO_2.

2.2. Compounds

The Pandemic Response Box (containing 400 structurally diverse drug-like compounds) was kindly provided by the MMV Foundation. The compounds were supplied in five 96-well plates A – E. A total of 80 wells in each plate contained 10 μL/well of 10 mM compound (dissolved in DMSO) except for Plate E which had 10 μL/well of 2 mM compound (dissolved in DMSO) in the last 11 wells. All plates were stored at −20 °C. The MMV compound IDs for the 400 compounds are provided in Table S1.

Compounds 1 (MolPort-001-816-819), 2 (MolPort-003-723-761), 3 (MolPort-005-982-777), and 4 (MolPort-007-995-593) were sourced via MolPort. These compounds were used in this study because of their structural similarity to the one compound of interest from the Pandemic Response Box screen. Compounds 1, 2, 3, and 4 were purchased as powders with 97%, >90%, >90%, and 95% purity, respectively, and were diluted in DMSO to a final concentration of 100 mM, 50 mM, 50 mM, and 100 mM, respectively. All compounds were stored at −20 °C after dissolving in DMSO.

2.3. Cell viability assay

Cell viability and cytotoxicity were assessed using the resazurin cell viability assay. TREx-BCBL-1-RTA or BC-1 cells were seeded at a density of 4×10^5 cells/mL in medium in wells of a flat 96-well tissue culture plate and treated with compound(s) or DMSO (as vehicle control) for 22 h. For HEK293T cells, cells were seeded at a density of 1.5×10^5 cells/mL in medium in wells of a flat 96-well tissue culture plate for 16 h before treatment (to allow the cells enough time to attach to the plate). The cells were treated with compound(s) or DMSO (as vehicle control) for 22 h. Resazurin dye (7-hydroxy-3H-phenoxazin-3-one 10-oxide) was added to the cells and incubated at 37 °C for 2 h. The amount of resorufin produced (which is proportional to the number of viable cells) was determined by measuring the fluorescence intensity at an excitation wavelength of 560 nm and emission wavelength of 590 nm. The relative cell viability for the treated cells was calculated as a fraction or percentage of fluorescence reading for treated cells to fluorescence reading for the DMSO control. For CC_{50} determination, the fluorescence readings for the treated cells were used to plot a dose-response curve via non-linear regression in GraphPad Prism software.

2.4. ELISA-based assay for measuring KSHV ORF57 protein in lysates

Reactivated and unreactivated TREx-BCBL-1-RTA cells in suspension were lysed using 10x lysis buffer [1.5 M NaCl, 10% (v/v) Triton X-100, 10% (w/v) Sodium deoxycholate, 1% (w/v) SDS, 100 mM Tris-Cl (pH

7.5), and 10x cOmplete™ EDTA-free protease inhibitor cocktail (Sigma-Aldrich, Germany)] on ice for 25 min. A total of 50 μL of the whole cell lysates were pipetted into designated wells of 2 separate 96-well flat-bottom high binding microtitre plates (Greiner Bio-One, Germany) and incubated at 4 °C for 16 h. Non-specific binding sites in the wells were blocked with 3% (w/v) BSA at 22 °C for 2 h. Monoclonal mouse anti-ORF57 (Santa Cruz, sc-135746) and polyclonal rabbit anti-GAPDH (Santa Cruz, sc-25778) primary antibodies with HRP-conjugated donkey anti-mouse IgG (Thermo Fisher Scientific, A16011) and HRP-conjugated donkey anti-rabbit IgG (Thermo Fisher Scientific, A16023) secondary antibodies were used for detecting KSHV ORF57 and GAPDH proteins, respectively. HRP buffer (pH 5) [25.7 mM citric acid, 48.6 mM Na_2HPO_4, 1 mg/mL TMB (in DMSO), and 30 % (v/v) H_2O_2.] was added into each well and incubated at 25 °C for 15 min in the dark for colour development. The reaction was stopped by adding 1 M H_2SO_4 and absorbance read at 450 nm. The absorbance reading was proportional to the amount of KSHV ORF57 or GAPDH protein present in the cell lysates.

2.5. Western blotting

Reactivated TREx-BCBL-1-RTA, BC-1 or rKSHV.219 cells were treated with either DMSO (as reactivated untreated control) or compounds and unreactivated TREx-BCBL-1-RTA or BC-1 cells were treated with DMSO (as unreactivated untreated control) for 24. The cells were washed with ice-cold phosphate-buffered saline (pH 7.45) and collected by centrifugation. Lysis buffer [150 mM NaCl, 1% (v/v) Triton X-100, 1% (w/v) Sodium deoxycholate, 0.1% (w/v) SDS, 10 mM Tris-Cl (pH 7.5), and 1x cOmplete™ EDTA-free protease inhibitor cocktail (Sigma-Aldrich, Germany)] was used to extract protein samples on ice for 25 min from cell pellets. The concentration of protein in lysates was determined using the bicinchoninic acid (BCA) protein quantification assay as described by Smith et al. (1985) with modifications (Smith et al., 1985) and denatured in Laemmli SDS loading buffer at 95 °C for 5 min. An equal amount of denatured protein samples was resolved by SDS-PAGE and transferred to nitrocellulose membrane using the complete Bio-Rad Trans-Blot Turbo Transfer System (BioRad, California, USA). The nitrocellulose membrane was blocked in 5% (w/v) Blotto, non-fat dry milk (Santa Cruz Biotech., CA, USA) dissolved in Tris-buffered saline containing 0.1% Tween-20 (TBST). The membrane was incubated in the appropriate primary and secondary antibodies. The primary antibodies used in this study were mouse anti-ORF57 (207.6) monoclonal antibody (Santa Cruz Biotechnology, sc-135746), HRP-conjugated anti-GAPDH antibody (EPR6256) (Abcam, ab185059), mouse anti-KSHV ORF45 (2D4A5) (Novus Biologicals, NPB2-37685), and mouse anti-EBV EBNA-1 (1EB12) monoclonal antibody (Santa Cruz Biotechnology, sc-81581). The secondary antibodies used in this study were HRP-conjugated donkey anti-mouse IgG (Thermo Fisher Scientific, A16011) and HRP-conjugated donkey anti-rabbit IgG (Thermo Fisher Scientific, A16023) secondary antibodies. Visualization of blots was performed using the Clarity™ Western ECL substrate kit (BioRad, California, USA) and image capture performed using a BioRad ChemiDoc™ MP System (BioRad, California, USA).

2.6. Determination of viral mRNA transcript expression levels

Cellular and viral mRNA were extracted from TREx-BCBL-1-RTA, BC-1, rKSHV.219 or HEK293T cells (for re-infection assays) to determine viral transcription levels. Reactivated TREx-BCBL-1-RTA or BC-1 cells were treated with either DMSO (as reactivated untreated control) or compounds and unreactivated TREx-BCBL-1-RTA or BC-1 cells were treated with DMSO (as unreactivated untreated control) for 24–48 h HEK293T cells were treated with either DMSO (as untreated control), compounds or viral supernatants for 24 h. Reactivated rKSHV.219 cells were treated with either DMSO (as untreated control) or compounds and unreactivated rKSHV.219 cells were treated with DMSO (as unreactivated untreated control) for 24 h. Total RNA was extracted from the cells using Zymo Research Direct-zol™ RNA Miniprep Plus kit (Zymo Research, cat. No.: R2073) according to the manufacturer's instructions. The extracted RNA was subjected to RNA clean-up and concentration to remove viral and/or genomic DNA contamination through DNase I treatment using the Zymo Research RNA Clean and Concentrator™-5 kit (Zymo Research, Catalogue number: R1014) according to the manufacturer's instructions. The resultant cleaned-up and concentrated RNA was reverse transcribed to cDNA using the LunaScript® RT SuperMix kit (New England Biolabs, cat. No.: E3010L) according to the manufacturer's instructions. The cDNA was subjected to qPCR analysis to determine the expression levels of viral mRNA transcripts relative to human GAPDH mRNA transcript (used as a normalizer). The oligonucleotide primer sets used in this study for qPCR were purchased from Integrated DNA Technologies. The forward and reverse sequences for the primers are: ORF57 (5′-CACTTCTGGAATACTACAGGCCAGG-3'; 5′-GTTAAATTTGGCCGACCCCATTGC-3′), ORF47 (5′-CGCGACCACTGCAGATAGCTCTATTC-3'; 5′-TTCCCTTTTGACCTGCGTGCG-3′), ORF65 (5′-CCTTAGGGATCAGAAACCGCGC-3'; 5′-CAGAGGACAGGGTGGTTATACTGC-3′), ORF45 (5′-CCGCCCACTCGATTTCATCAGG-3'; 5′-TCCAGCCACGGCCAGTTATATGC-3′), ORFK8 (5′- GTCATCGAAAGCATACACAAGACAGC-3'; 5′- TGCTGGCACATTCGCATCAGC-3′), ORF10 (5′- ATC TCTAATCGAGTACCCCT-3'; 5′- TAGAATGCAGTGTAGGTCTC-3′), ORF 52 (5′- ACCTTGCTGAATATTGTCCT-3'; 5′- CCTTACGATGGAAGAC CTAA-3′), ORF62 (5′- GTTCCCTTTGATTCTCATCCGGTGC-3'; 5′-CAGAAACACAGTCCAGGGGCC-3′), ORF50 (5′-AGACCCGGCGTTTATTAGTACGT-3'; 5′-CAGTAATCACGGCCCCTTGA-3′), ORF73 (5′- CCAGACCAGTCGCCCATAACTTATTG-3'; 5′-GGAAGATTGTAGGTTTCCTGC CAGG-3′), vIRF3 (5′-AGCCGTACACTGTGTTGATAC-3'; 5′-CACGATTCATAGTGAGAAACA-3′), and GAPDH [Hs.PT.39a.22214836 (5′-ACA TCGCTCAGACACCATG-3'; 5′-TGTAGTTGAGGTCAATGAAGGG-3′)].

The expression levels of cellular and viral target genes were determined by two-step quantitative reverse transcription PCR (qPCR) using a CFX Connect Real-Time PCR Detection System (Bio-Rad, SA). For all qPCR experiments, the appropriate number of controls and replicates were included to conform with the minimum information for publication of quantitative real-time PCR experiments (MIQE) guidelines (Bustin et al., 2009). The qPCR reaction component for each test sample included 10 μL of Luna® Universal qPCR Master Mix (New England Biolabs, cat. No.: M3003E), 0.5 μL of 10 μM forward primer, 0.5 μL of 10 μM reverse primer, either 10 ng of template genomic DNA (variable volume) or 50 ng of reverse transcriptase (RT) cDNA template (variable volume) and nuclease-free water (to make up mixture volume to 20 μL). The qPCR reaction component for each control sample included 10 μL of Luna® Universal qPCR Master Mix, 0.5 μL of 10 μM forward primer, 0.5 μL of 10 μM reverse primer, either nuclease-free water (equal volume of template genomic DNA used) or 50 ng of no reverse transcriptase (NRT) cDNA template (variable volume) and nuclease-free water (to make up mixture volume to 20 μL). The thermocycling protocol was a 60 s initial denaturation step at 95 °C, followed by 40 cycles of 15 s denaturation step at 95 °C and 30 s extension step at 60 °C. A melt curve analysis was performed at a 0.2 °C increment from 60 to 95 °C to confirm that a single specific product was amplified. At the end of the qPCR run, the data were acquired and analysed using the CFX Maestro Software (Bio-Rad, SA). Each target gene C_T value was normalized to GAPDH (the housekeeping gene) and was quantified using the comparative C_T ($\Delta\Delta C_T$) method as described by Schmittgen and Livak (2008) (Schmittgen and Livak, 2008). Viral transcript levels in the treated reactivated TREx-BCBL-1-RTA or BC-1 or infected HEK293T cells were compared to the viral transcript levels in the reactivated DMSO control or uninfected HEK293T cells.

2.7. Viral DNA replication assay

The viral DNA replication assay was performed to monitor KSHV replication within the host cell upon induction of lytic reactivation in

treated and untreated cells. Reactivated TREx-BCBL-1-RTA cells were treated with either DMSO (as reactivated untreated control) or compounds and unreactivated TREx-BCBL-1-RTA cells were treated with DMSO (as unreactivated untreated control) for 72 h. Total genomic DNA was extracted from the cells using the Zymo Research *Quick*-DNA™ Miniprep kit (Zymo Research, cat. No.: D3025) according to the manufacturer's instructions. An amount of 10 ng of template genomic DNA was used for qPCR analysis with primers specific to KSHV ORF57 gene (to assess the level of viral DNA) and human GAPDH gene (as the normalizer). Viral DNA level in treated reactivated TREx-BCBL-1-RTA cells was compared to the viral DNA level in the reactivated DMSO control.

2.8. KSHV re-infection assays

The KSHV re-infection assays were performed with TREx-BCBL-1-RTA cells (KSHV infected cell line capable of producing infectious virion particles) and HEK293T cell line (target host cells for re-infection) to monitor the production of infectious virions or viral entry. For re-infection assays to determine infectious virion production. Reactivated TREx-BCBL-1-RTA cells treated with DMSO (as untreated control) or compound(s) and unreactivated TREx-BCBL-1-RTA cells treated with DMSO (as untreated control for reactivation) were cultured for 72 h. The viral supernatants were used to infect naïve HEK293T cells and to determine viral load in the supernatants. A 2.7 mL volume of each viral supernatant was mixed with 300 μL of complete DMEM (HEK293T growth medium) and the mixture was used to infect HEK293T cells (that had been seeded in a 6-well plate a day before) for 24 h. Total RNA was extracted from the HEK293T cells, treated with DNase I, reverse transcribed to cDNA, and qPCR analysis was used to determine the expression level of KSHV ORF57 and ORF73 mRNA transcripts in the HEK293T cells as an indication of viral infection (Murphy et al., 2023; Schumann et al., 2016). A 2 μL volume of each viral supernatant was used for qPCR analysis with primers specific to KSHV ORF57 gene. The amount of KSHV DNA in ng was determined from a standard curve and converted to copy number using the equation (ng RNA x 6.022×10^{23})/(length x 1×10^{9} x 660) and used to normalise the amount of virus in each re-infection assay.

For re-infection assays to determine infectious viral entry, unreactivated and reactivated TREx-BCBL-1-RTA cells were cultured for 72 h. A 2.7 mL volume of each viral supernatant was mixed with 300 μL of complete DMEM (HEK293T growth medium). The reactivated viral supernatant was supplemented with DMSO (as untreated control) or compound(s) while the unreactivated supernatant was treated with DMSO (as untreated control for reactivation). The treated supernatant was immediately used to infect HEK293T cells that had been seeded in a 6-well plate a day before. Total RNA was extracted from the HEK293T cells, treated with DNase I, reverse transcribed to cDNA and qPCR analysis was used to determine the expression level of KSHV ORF57 mRNA transcript in the HEK293T cells as an indication of viral infection.

2.9. Reproducibility and statistical analysis

Western blot analyses were performed at least three independent times and densitometry data for the western blots are the mean ± SEM of at least three independent biological replicates, except where otherwise stated. All qPCR data are the mean ± SEM of experiments performed in technical triplicates and are a representation of at least two independent biological replicates with similar trends. The data for ELISA-based and cell viability assays are the mean of experiments performed in technical triplicates and are a representation of at least two independent biological replicates, except where otherwise stated. The IC_{50} and CC_{50} data are the mean ± SEM of experiments performed in technical triplicates and are a representation of at least two independent biological replicates. The graphs/curves and statistical analyses performed in this study were plotted using GraphPad Prism software version 9 (GraphPad Software Inc., CA, USA).

3. Results

3.1. Development of a medium-throughput phenotype-based screening assay

Prior to screening, an ELISA-based medium-throughput screening assay to determine KSHV ORF57 protein levels relative to the host GAPDH protein and cell viability from the same sample was developed (Fig. 1A). The primary and secondary antibody dilutions were optimized (Fig. S1A), and the impact of FBS in the growth medium on KSHV ORF57 protein detection and TREx-BCBL-1-RTA cell viability was assessed. The impact of resazurin dye used for viability assessment on KSHV ORF57 protein detection was also assessed (Fig. S1). Given that TREx-BCBL-1-RTA is a suspension cell line and must be lysed in growth medium the impact of FBS on KSHV ORF57 protein detection was assessed. FBS-supplemented medium negatively impacted the detection of KSHV ORF57 protein level between reactivated and unreactivated samples (Fig. S1B), suggesting serum in the FBS-supplemented medium reduced the resolution of KSHV ORF57 protein detection. Also, whole cell lysate protein concentrations from cells grown in FBS-supplemented medium were at least 3.3-fold higher than those grown in FBS-free medium regardless of the cell seeding density (Fig. S1C, Table S2). This suggested that serum may compete with cellular and viral proteins for binding to ELISA plates.

KSHV ORF57 protein levels in TREx-BCBL-1-RTA cells were similar at 8- and 24-h post-induction of lytic replication irrespective of the presence of FBS, the exclusion of which did not affect the induction of KSHV lytic replication and/or the expression of lytic proteins after 24 h (Fig. S1D). This time (24 h) was also sufficient to discriminate between KSHV ORF57 protein levels in reactivated and unreactivated TREx-BCBL-1-RTA cells (Fig. S1E). The cell viability test confirmed that the TREx-BCBL-1-RTA cells were viable in FBS-free medium within 24 h under both latent and lytic conditions (Fig. S1F).

Given that the screening approach was based on the inhibition of KSHV ORF57 protein expression (as a marker for KSHV lytic replication) and cytotoxicity of the MMV compounds in the same population of reactivated TREx-BCBL-1-RTA cells in suspension, the impact of resazurin cell viability dye on KSHV ORF57 protein detection using the ELISA-based assay was assessed. Although resazurin dye reduced KSHV ORF57 detection in TREx-BCBL-1-RTA cells in FBS-free medium (Fig. S1G), the effect was minor and still permitted sufficient resolution of differences between the reactivated and unreactivated samples. Additionally, determining the cytotoxicity and KSHV ORF57 protein inhibition of each MMV compound from the same population of cells from the same 96-well plate would prevent the variations that splitting of cells into two different 96-well plates would introduce.

Therefore, the final assay used 8×10^{4} TREx-BCBL-1-RTA cells cultured in 200 μL of FBS-free medium (at a seeding density of 4×10^{5} cells/mL) in 96-well plates and treated with DOX to induce lytic replication for 24 h. The final optimized assay antibody conditions discriminated between KSHV ORF57 protein levels in reactivated and unreactivated TREx-BCBL-1-RTA cell lysates. The cytotoxicity of each MMV compound and the respective KSHV ORF57 protein level were determined from the same population of cells seeded in wells of the same 96-well plate.

3.2. Screening of the pandemic response box for non-cytotoxic inhibitors of KSHV ORF57 protein expression

The 400 MMV Pandemic Response Box compounds were screened for non-cytotoxic inhibitors of KSHV ORF57 protein expression as a marker for KSHV lytic replication at a 20 μM single-point screening concentration (Fig. 1A). The inhibition of KSHV ORF57 protein expression was expressed as a fraction of KSHV ORF57 protein level normalized to

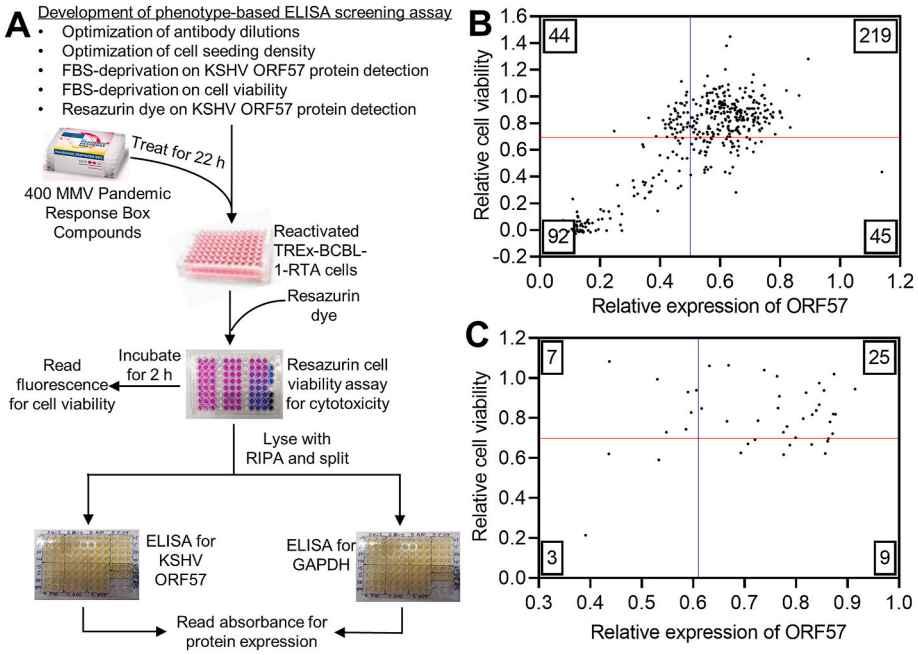

Fig. 1. Screening of MMV Pandemic Response Box for inhibitors of KSHV ORF57 protein. (A) Optimized workflow for the medium-throughput phenotypic ELISA and cell viability screening assays. **(B)** Reactivated TREx-BCBL-1-RTA cells were treated with 400 MMV compounds at a single-point screening concentration of 20 μM for 24 h. The relative expression of KSHV ORF57 protein normalized to GAPDH, and relative cell viability were determined using an ELISA-based assay and resazurin cell viability assay from the same population of treated reactivated TREx-BCBL-1-RTA cells. A total of 44 compounds, represented by the data points in the top left quadrant, met the selection criteria, namely a cut-off of relative cell viability of 0.7 (indicated by the red line) and a relative ORF57 expression level of 0.5 (indicated by the blue line). **(C)** Reactivated TREx-BCBL-1-RTA cells were treated with the selected 44 MMV compounds at a single-point concentration of 10 μM for 24 h. The relative expression of KSHV ORF57 protein normalized to GAPDH, and relative cell viability were determined using the ELISA-based assay and resazurin cell viability assay from the same population of treated reactivated TREx-BCBL-1-RTA cells. Only 7 compounds, represented by the data points in the top left quadrant, met the selection criteria, namely a cut-off of relative cell viability of 0.7 (indicated by the red line) and a relative ORF57 expression level of 0.606 (indicated by the blue line). The data shown are the mean of a single independent experiment performed in technical duplicate.

GAPDH in treated reactivated cells to KSHV ORF57 protein level normalized to GAPDH in the reactivated DMSO control cells. The relative cell viability of each MMV compound was expressed as a fraction of the fluorescence reading of the treated reactivated cells to the fluorescence reading of the reactivated DMSO control cells. The initial screening selection criteria were KSHV ORF57 relative expression less than or equal to 0.5 and a relative cell viability value greater than or equal to 0.7, with 44 compounds, represented by the data points in the top left quadrant of the graph, meeting the selection criteria (Fig. 1B–Table S1). There were a further 219 compounds that were non-cytotoxic, but which did not supress relative expression of KSHV ORF57 below the 0.5 threshold. A total of 45 cytotoxic compounds had a KSHV ORF57 relative expression greater than 0.5, and 92 compounds that were cytotoxic with KSHV ORF57 relative expression less than 0.5. These compounds were all excluded (Fig. 1B–Table S1). Of the 153 compounds in the Pandemic Response Box with reported antiviral activity, there were 10 compounds with reported anti-herpesvirus activity. None of the 10 compounds with reported anti-herpesvirus activity met the selection criteria for the initial screening presumably because most of these compounds target later phases in the KSHV replication cycle. MMV690653 [letermovir (70% cell viability)], MMV001761 [ganciclovir (92% cell viability)], MMV001961 [acyclovir (84% cell viability)], MMV1580486 [pritelivir (100% cell viability)], MMV1580478 [tenofovir (100% cell viability)] and MMV1782210 [cyclopropavir (91% cell viability)] were non-cytotoxic to reactivated TREx-BCBL-1-RTA cells but the percentage inhibition of KSHV ORF57 protein ranged from 30 to 43% which was below the selection criterion of 50%. MMV009948 [imatimib (38% cell viability)], MMV639951 [everolimus (33% cell viability)], and MMV1580493 [verdinexor (12% cell viability)] showed high percentage KSHV ORF57 protein inhibition (65%, 53%, and 73%, respectively) but this was attributed to cytotoxicity. MMV1593517 [selinexor (63% cell viability and 35% KSHV ORF57 inhibition)] did not meet any of the selection criteria (Table S1). Interestingly, only 4 compounds (MMV1645152, MMV1782222, MMV1580499, and MMV1634394) out of the 153 compounds in the Pandemic Response Box with reported antiviral activity were among the 44 compounds that met the initial selection criteria (Table S1)

The 44 compounds meeting our initial selection criteria, were further triaged by a single-point screen at 10 μM. Here selection criteria were modified to KSHV ORF57 relative expression of less than or equal to 0.606 and a relative cell viability value greater than or equal to 0.7. This reduced the cohort to 7 potential non-cytotoxic inhibitors of KSHV lytic replication, represented by the data points in the top left quadrant of the graph (Fig. 1C–Table S3). From these data, MMV1645152 was shown to have the lowest relative KSHV ORF57 protein expression value (0.437) and the highest relative cell viability value (1.082) (Table S3).

3.3. MMV1645152 is the most active non-cytotoxic inhibitor of KSHV ORF57 expression

The selected 7 compounds from the validation screening were MMV1645152, MMV1782223, MMV1634394, MMV1634403, MMV1782212, MMV1634363, and MMV1578568 (Fig. 2A). Western blot analysis was subsequently used as an orthogonal method to validate these compounds for non-cytotoxic reduction in KSHV ORF57 expression at a 50 μM single-point treatment concentration. The Western blot data indicated that MMV1645152 was the most potent inhibitor of KSHV ORF57 expression (Fig. 2B), with no observable cytotoxicity at 50 μM, and subsequently the most favourable selectivity index (calculated as relative cell viability/relative expression of KSHV ORF57, Table 1). MMV1782212 was cytotoxic resulting in at least 97% cell death at 50

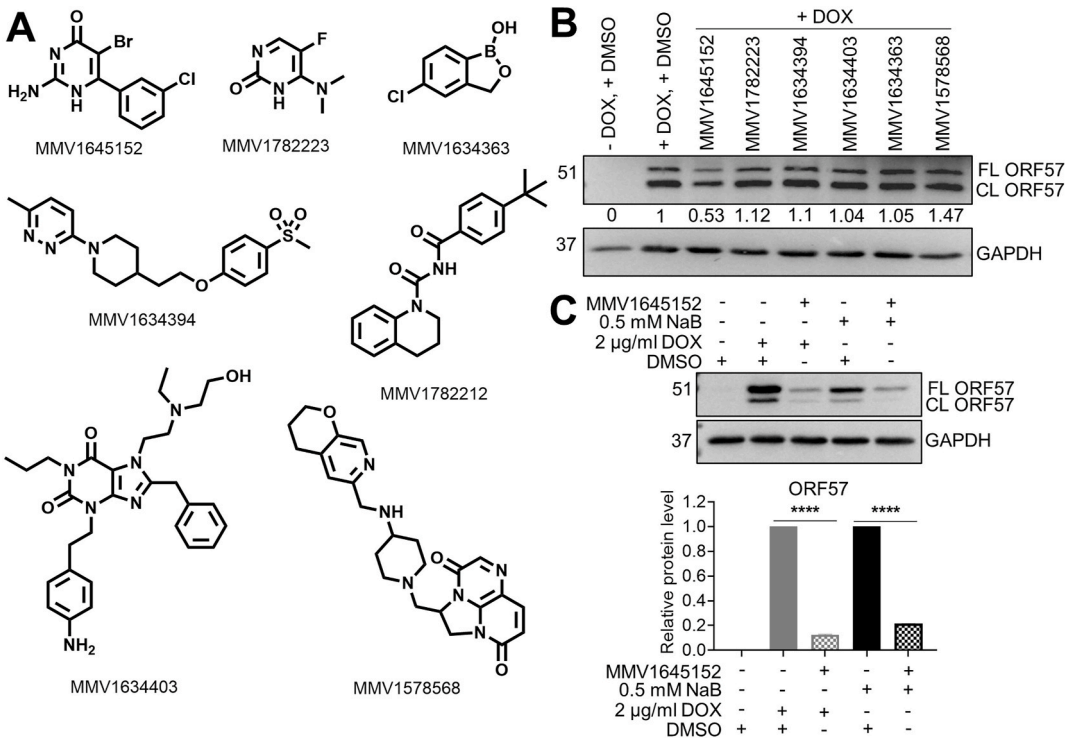

Fig. 2. MMV1645152 is the best inhibitor of KSHV ORF57 protein (A) Structure of the selected 7 MMV compounds. **(B)** Western blot analysis of KSHV ORF57 protein in reactivated TREx-BCBL-1-RTA cells treated with 50 μM of 6 of the 7 MMV compounds (excluding the cytotoxic MMV1782212) for 24 h. The number under each lane of the top blot represents the relative expression of KSHV ORF57 protein normalized to GAPDH for experiment performed once. The normalized expression of KSHV ORF57 protein in each sample was relativized to the reactivated DMSO control. **(C)** Western blot analysis and corresponding densitometry (using Image J) of KSHV ORF57 protein in TREx-BCBL-1-RTA cells reactivated with either 2 μg/mL DOX or 0.5 mM sodium butyrate (NaB) and treated with 50 μM MMV1645152 for 24 h. FL and CL ORF57 indicate the full-length and cleaved ORF57, respectively. Both the FL and CL ORF57 were quantified for all KSHV ORF57 densitometry analysis in this study. The normalized expression of KSHV ORF57 protein in each treated sample was relativized to the corresponding reactivated DMSO control. Unreactivated TREx-BCBL-1-RTA responses are indicated by -DOX and -NaB. Statistical analysis comparing each treated sample to their corresponding reactivated DMSO control was determined by unpaired student's t-test in GraphPad Prism where $^{****}P < 0.0001$ was considered significant.

Table 1
Screening data for the 7 selected MMV compounds.

MMV Compound ID	Relative expression of KSHV ORF57[a]	Relative cell viability	Selectivity index
MMV1645152	**0.53**	**1.028**	**1.940**
MMV1782223	1.12	0.783	0.700
MMV1634394	1.1	0.73	0.664
MMV1634403	1.04	0.535	0.514
MMV1782212	N/A	0.027	N/A
MMV1634363	1.05	0.844	0.804
MMV1578568	1.47	0.751	0.511

[a] From Western blot in Fig. 2B.

μM (Table 1). Consequently, an insufficient amount of cellular protein was available for Western blot analysis.

As a further control, we sought to exclude the potential contribution of doxycycline (DOX, used to induce lytic replication) to the anti-KSHV activity of MMV1645152 by using NaB as an alternative inducer of KSHV lytic replication (Sandhu and Damania, 2022). Firstly, the maximum concentration of NaB required to cause a similar percentage of cell death as 2 μg/mL DOX in TREx-BCBL-1-RTA cells was determined (83.4% and 84.7%, respectively) (Fig. S2). Therefore, 0.5 mM NaB and 2 μg/mL DOX were used to induce KSHV lytic replication in TREx-BCBL-1-RTA cells in the presence of 50 μM MMV1645152. DOX induced a more robust KSHV lytic replication than 0.5 mM NaB (Fig. 2C). However, the relative reduction in expression of KSHV ORF57 protein in the DOX- and NaB-reactivated TREx-BCBL-1-RTA cells with 50 μM MMV1645152 was similar (Fig. 2C), indicating that DOX did not contribute to the inhibition of KSHV ORF57 protein expression by MMV1645152.

Next, the IC_{50} and CC_{50} of the identified 7 MMV compounds were determined. In this study, the IC_{50} refers to the concentration of a compound required to inhibit KSHV ORF57 protein expression by 50% when compared to the untreated control, while CC_{50} indicates half-maximal cytotoxicity concentration. The IC_{50}, CC_{50}, and selectivity indices (CC_{50}/IC_{50}) again showed that MMV1645152 was the most promising compound (Table 2, Figs. S3A and S3B). Although MMV1782212 had similar selectivity index to MMV1645152 (0.860 and 0.865, respectively), it was more cytotoxic (Table 2, Fig. S3B). Taken together, these data suggested that MMV1645152 is the most promising non-cytotoxic inhibitor of KSHV ORF57 protein expression in MMV Pandemic Response Box.

3.4. MMV1645152 is a superior inhibitor of KSHV ORF57 protein and lytic gene expression than the structural analogues of MMV1645152

Next, the dose dependent inhibition of KSHV ORF57 protein

Table 2
IC_{50}, CC_{50}, and selectivity index of the selected 7 MMV compounds.

MMV Compound ID	IC_{50} (μM)	CC_{50} (μM)	Selectivity index
MMV1645152	**132.7**	**114.8**	**0.865**
MMV1782223	>200	15.7	<0.079
MMV1634394	179.9	37.7	0.21
MMV1634403	122.1	47	0.385
MMV1782212	8.8	7.6	0.86
MMV1634363	205.7	52.9	0.257
MMV1578568	231.3	67.8	0.293

expression by MMV1645152 was evaluated and compared to that of selected structural analogues of MMV1645152. MMV1645152 inhibited KSHV ORF57 protein expression in a dose-dependent manner with a significant reduction in KSHV ORF57 protein level at 20 μM treatment concentration and above (Fig. 3A). The dose-response curves derived from the Western blot showed that the IC_{50} of MMV1645152 for KSHV ORF57 protein expression were estimated to be 17.1 μM (Fig. S4). The IC_{50} of MMV1645152 determined using ELISA (Table 2) and Western blot analysis (Fig. S4) varied because the ELISA technique has lower resolution, specificity and sensitivity compared to Western blot. Hence, we regarded the IC_{50} from the Western blot as more accurate and so a range of concentrations around that value were used in subsequent studies. These concentrations were also below the CC_{50} value such that we were able to retain above 80% cell viability in all assays.

The activity of four commercially available structural analogues of MMV1645152 (Compound **1**–**4,** Fig. 3B) was compared to MMV1645152. While all four compounds were less cytotoxic than MMV1645152 (Figs. S5A–D and S3B), compounds **1, 2**, and **3** had no discernible effect on KSHV ORF57 protein expression, while compound **4** demonstrated weaker albeit dose-dependent inhibitory activity (Fig. 3C and D). Together this tentatively indicated the importance of both the position of the aryl halogenation and the presence of the amino pyrimidinone bromine substituent on MMV1645152 (Figs. 2A and 3A-D).

Next, we determined whether MMV1645152 inhibited another immediate early lytic protein (KSHV ORF45) in a dose-dependent manner. The effect of MMV1645152, the inactive control (compound 1) and partially active control (compound 4) structural analogues on the expression of KSHV ORF45 was investigated using Western blot. Neither MMV1645152 nor the selected structural analogues significantly altered KSHV ORF45 protein levels in reactivated TREx-BCBL-1-RTA cells (Fig. 3E). Taken together, these suggested that MMV1645152 specifically inhibits KSHV ORF57 protein.

We next evaluated the gene expression levels of the immediate early

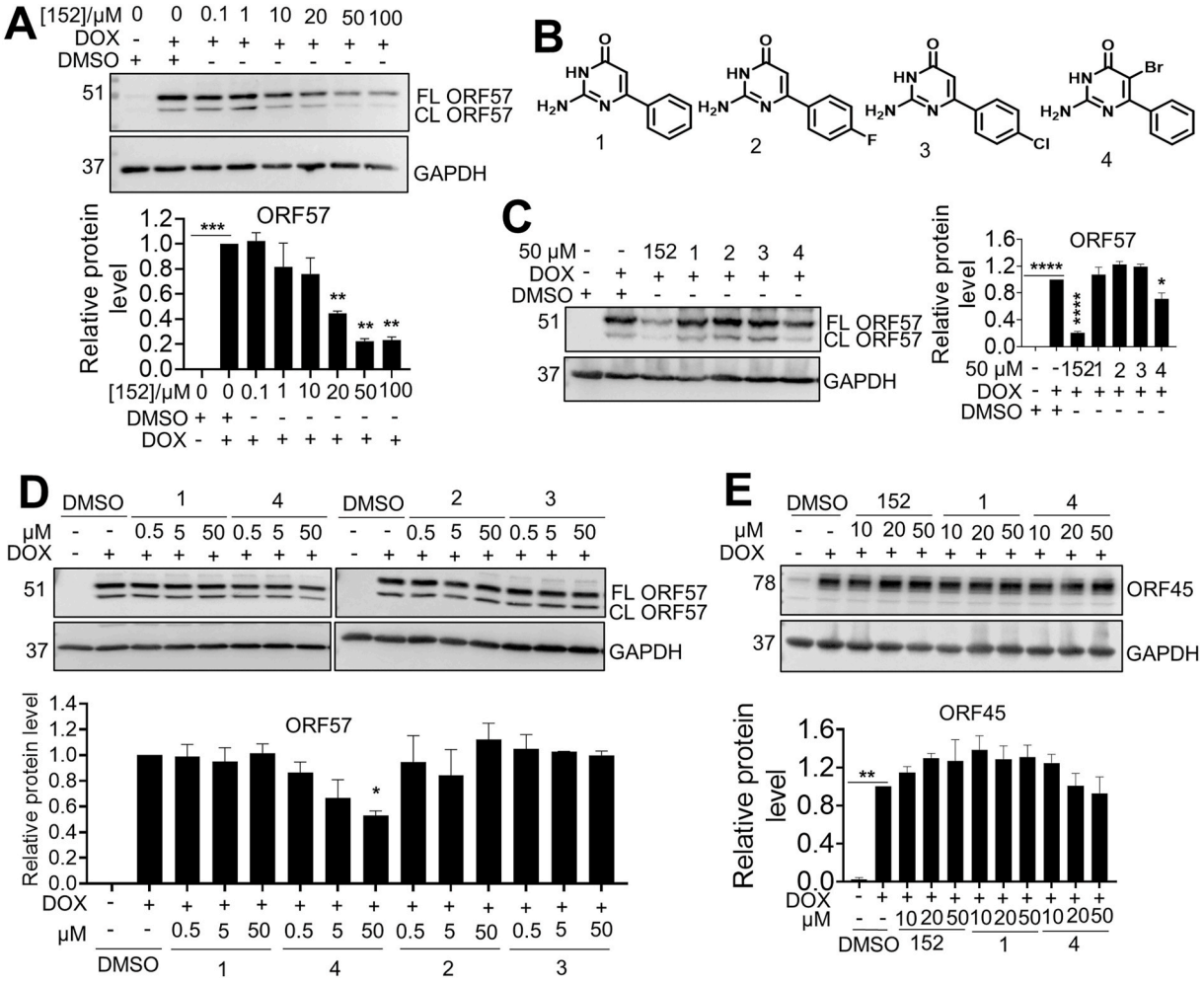

Fig. 3. MMV1645152 is more effective at inhibiting KSHV ORF57 protein expression than the structural analogues of MMV1645152 (A) Western blot analysis and corresponding densitometry (using Image J) of KSHV ORF57 protein in reactivated TREx-BCBL-1-RTA cells treated with increasing concentrations (0–100 μM) of MMV1645152 for 24 h. The normalized expression of KSHV ORF57 protein in each sample was relativized to the reactivated DMSO/untreated control. **(B)** Structural analogues of MMV1645152. **(C)** Western blot analysis and corresponding densitometry (using Image J) of KSHV ORF57 protein in reactivated TREx-BCBL-1-RTA cells treated with 50 μM MMV1645152 or 50 μM of each analogue for 24 h. The normalized expression of KSHV ORF57 protein in each sample was relativized to the reactivated DMSO control. **(D)** Western blot analysis and corresponding densitometry (using Image J) of KSHV ORF57 protein in reactivated TREx-BCBL-1-RTA cells treated with increasing concentrations (0–50 μM) of each analogue for 24 h. The normalized expression of KSHV ORF57 protein in each sample was relativized to the reactivated DMSO control. **(E)** Western blot analysis and corresponding densitometry (using Image J) of KSHV ORF45 protein in reactivated TREx-BCBL-1-RTA cells treated with increasing concentrations (0–50 μM) of MMV1645152 or compound 1 or compound 4 for 24 h. The normalized expression of KSHV ORF45 protein in each sample was relativized to the reactivated DMSO control. Unreactivated TREx-BCBL-1-RTA responses are indicated by -DOX. Statistical analysis comparing each treatment concentration to the reactivated DMSO control was determined by one-way ANOVA with Dunnett's multiple comparisons test where $^{*}P < 0.05$, $^{**}P < 0.01$, $^{***}P < 0.001$, and $^{****}P < 0.0001$ were considered significant.

lytic gene (KSHV ORF57), delayed early lytic gene (KSHV ORF47) and late lytic gene (KSHV ORF65) in reactivated TREx-BCBL-1-RTA cells treated with increasing concentrations of MMV1645152 or the inactive structural analogue (compound 1) or partially active structural analogue (compound 4) using qPCR (Fig. 4). MMV1645152, but not the structural analogues, significantly reduced KSHV ORF57 and ORF65 gene expression in a dose-dependent manner. MMV1645152 did not alter KSHV ORF47 gene expression. However, the structural analogues significantly increased KSHV ORF47 gene level in a dose-dependent manner (Fig. 4A–C). This suggested that reduced ORF57 levels with MMV1645152 also occurred at the transcript level.

Having shown that neither MMV1645152 nor the selected structural analogues altered KSHV ORF45 protein expression (Fig. 3E), we determined whether the compounds altered KSHV ORF45 transcript level in reactivated TREx-BCBL-1-RTA cells using qPCR. Neither MMV1645152 nor the selected structural analogues significantly altered KSHV ORF45 transcript level in reactivated TREx-BCBL-1-RTA cells (Fig. 4D). These data are consistent with the impact of the compounds on KSHV ORF45 protein expression (Fig. 3E). The gene expression levels of the early lytic gene (KSHV ORFK8) and late lytic genes (KSHV ORF10, ORF52, and ORF62) in reactivated TREx-BCBL-1-RTA cells treated with 50 μM MMV1645152 or the inactive structural analogue (compound 1) were also evaluated using qPCR. Neither MMV1645152 nor the inactive structural analogue significantly altered the gene expression level of KSHV ORFK8 at 50 μM (Fig. 4E). However, the gene expression of KSHV ORF10, ORF52, and ORF62 were significantly reduced by MMV1645152, in contrast no reduction was observed by the inactive analogue compound 1 (Fig. 4F–H).

KSHV ORF57 expression is upregulated by the KSHV latent-lytic switch transactivator (ORF50), therefore, to determine whether MMV1645152 or the inactive structural analogue (compound 1) blocked the expression of the KSHV ORF50, which then affected downstream ORF57 expression, qPCR was used to evaluate KSHV ORF50 expression in treated reactivated TREx-BCBL-1-RTA cells. Neither MMV1645152 nor compound 1 significantly inhibited the expression of KSHV ORF50 (Fig. 4I). This suggested that the anti-KSHV activities of MMV1645152 were not due to differential induction of KSHV lytic reactivation. In addition, MMV1645152 did not alter the expression of latent genes ORF73 and vIRF3 (Fig. S6) suggesting that MMV1645152 specifically targets KSHV during the lytic phase.

3.5. MMV1645152, but not the selected structural analogues, inhibits KSHV DNA replication in a dose dependent manner

The effect of MMV1645152 and the selected structural analogues on KSHV DNA replication was determined by assessing the levels of viral DNA, using primers specific to the KSHV ORF57 gene, relative to GAPDH gene in the host genome, as a marker for viral DNA replication. Treatment with DOX to induce lytic replication significantly increased viral DNA (Fig. 5A–C). KSHV DNA levels in reactivated TREx-BCBL-1-RTA cells were reduced in a dose-dependent manner with MMV1645152 (Fig. 5A), but not with the inactive analogue compound 1 (Fig. 5B) or the partially active analogue compound 4 (Fig. 5C). These data suggested that MMV1645152 blocked the expression of viral genes required for efficient viral DNA replication. The data also confirm that the anti-KSHV activity of MMV1645152 is specific.

3.6. MMV1645152 reduced production of infectious KSHV virions and inhibited viral infection of naïve HEK293T cells

To reduce KSHV infection, a therapeutic agent can either inhibit the production of infectious virus from infected cells or inhibit the entry of KSHV virions into host cells (or both). Accordingly, we conducted a re-infection assay to test both mechanisms (Fig. 6A). The CC_{50} concentrations of MMV1645152, compound 1, and compound 4 in HEK293T cells were first determined to be $>$ 500 μM, with at least 60% of the HEK293T cells still viable at 500 μM (Fig. S7). Consequently, a 50 μM treatment concentration was selected for the re-infection assays.

Reactivated TREx-BCBL-1-RTA cells were treated with 50 μM MMV1645152, compound 1 (Fig. 3B), or compound 4 (Fig. 3B) for 72 h and the viral supernatants were used to determine the levels of infectious KSHV virions. The level of KSHV ORF57 and ORF73 mRNA expression in HEK293T cells was normalized to the viral DNA load in the supernatants using qPCR (Fig. 6A). Treatment of reactivated TREx-BCBL-1-RTA cells with 50 μM MMV1645152 significantly reduced KSHV infection of HEK293T cells by 4-fold (when the lytic gene KSHV ORF57 was used as a marker) or 2-fold (when the latent gene KSHV ORF73 was used as a marker) (Fig. 6B and C). However, equivalent concentrations of compound 1 (inactive analogue) or compound 4 (partially active analogue) did not reduce infection of HEK293T cells by KSHV (Fig. 6B and C).

To determine whether MMV1645152 could directly inhibit KSHV lytic replication upon infection of naïve HEK293T cells, TREx-BCBL-1-RTA cells were reactivated for 72 h and the viral supernatants were supplemented with vehicle control (DMSO) or 50 μM compounds and immediately used to infect HEK293T cells for 24 h. The level of KSHV ORF57 mRNA in HEK293T cells was determined using qPCR (Fig. 6A). Only MMV1645152 significantly inhibited the lytic replication of KSHV upon infection of naïve HEK293T cells (Fig. 6D). Taken together, the re-infection data suggested that MMV1645152 inhibited viral infection through inhibition of KSHV infectious virion production and inhibition of KSHV lytic replication in naïve HEK293T cells.

3.7. MMV1645152, but not the inactive structural analogue, can inhibit KSHV lytic replication in the context of EBV co-infection

Having demonstrated that MMV1645152 possessed anti-KSHV activity in the TREx-BCBL-1-RTA cell line model of KSHV infection, we sought to investigate whether this activity could be replicated in another KSHV infected PEL cell line, namely the BC-1 cell line (a lymphoma cell line co-infected with KSHV and EBV).

The CC_{50} values for MMV1645152 and compound 1 (Fig. 3B) in reactivated BC-1 cells were 100.4 μM and 390.7 μM, respectively (Fig. S8). Compound 1 (inactive analogue) was less cytotoxic in BC-1 cells compared to MMV1645152; a trend similar to cytotoxicity in reactivated TREx-BCBL-1-RTA cells.

The impact of MMV1645152 and the inactive analogue control compound 1 on KSHV ORF57 protein expression was assessed using Western blot analysis. The expression of EBV EBNA-1 protein confirmed that the BC-1 cells are co-infected with KSHV and EBV. MMV1645152 significantly inhibited KSHV ORF57 protein expression in reactivated BC-1 cells in a dose-dependent manner (with at least 50% reduction at 10 μM) but did not significantly alter the expression level of EBNA-1. Compound 1 did not alter the expression level of KSHV ORF57 or EBV EBNA-1 (Fig. 7A). Furthermore, MMV1645152, but not the inactive analogue compound 1, significantly inhibited the expression of KSHV ORF57, ORF47 and ORF65 mRNA transcripts in a dose-dependent manner (Fig. 7B and C). Taken together, these data confirm that MMV1645152 can target KSHV in multiple KSHV infected cell lines, and in the context of EBV co-infection.

3.8. MMV1645152, but not the inactive structural analogue, can inhibit KSHV infection of immortalised epithelial cells

Having shown that MMV1645152 possessed anti-KSHV activity in lymphoma (TREx-BCBL-1-RTA and BC-1) cell lines, we sought to investigate if the anti-KSHV activity of MMV1645152 can be replicated in an immortalised epithelial model using HEK293T cells harbouring rKSHV.219 (Fig. 8).

The expression of KSHV ORF57 protein in rKSHV.219 cells treated with increasing concentrations of MMV1645152 or the inactive analogue control compound 1 was evaluated using Western blot

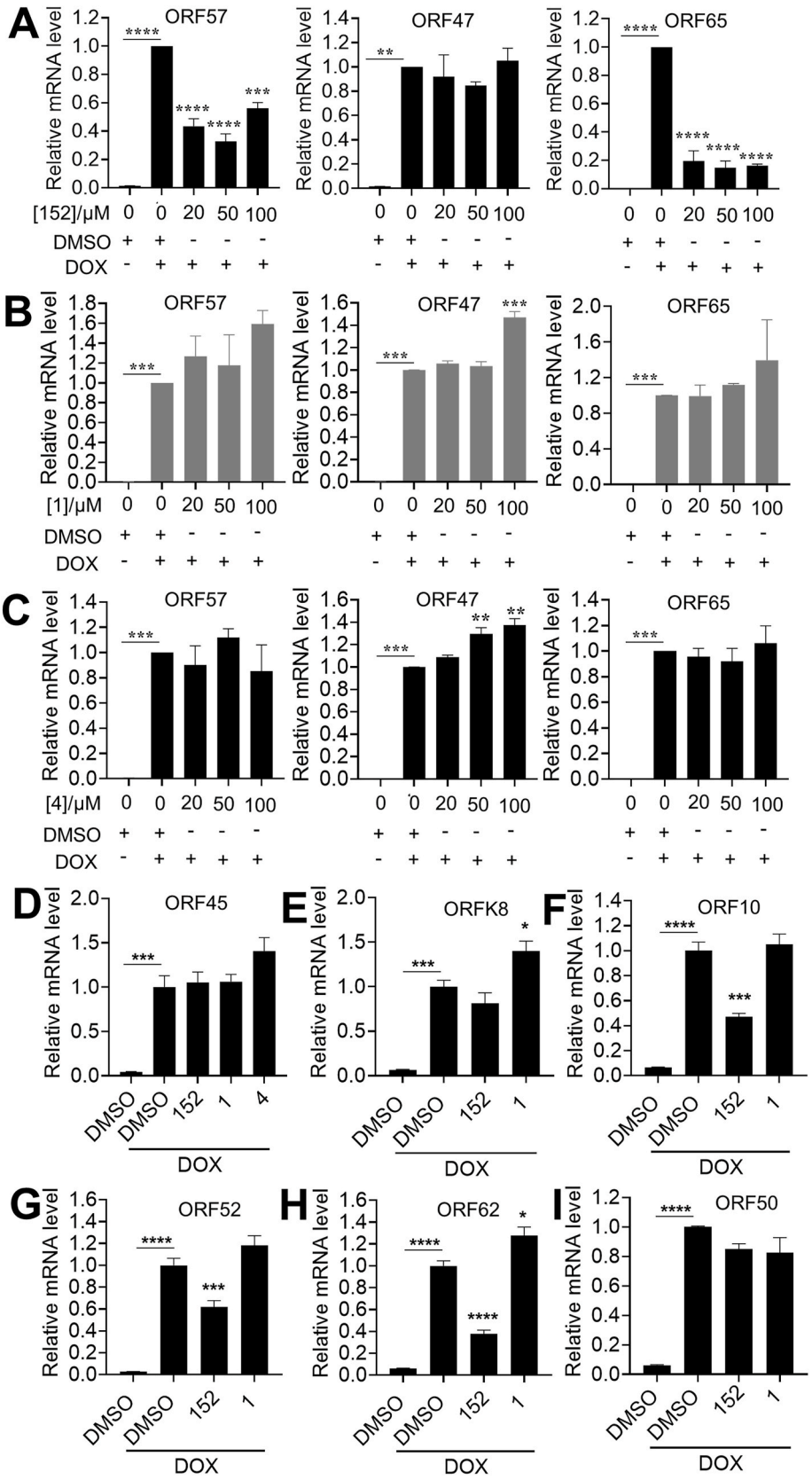

(caption on next page)

Fig. 4. MMV1645152 is more effective at inhibiting KSHV lytic genes than the selected structural analogues of MMV1645152. Reactivated TREx-BCBL-1-RTA cells were treated with increasing concentrations (0–100 μM) of **(A)** MMV1645152 or **(B)** compound 1 or **(C)** compound 4 for 24 h (for ORF57 analysis) or 48 h (for ORF47 and ORF65 analyses). qPCR analysis of KSHV ORF57, ORF47 and ORF65 mRNA transcripts normalized to host GAPDH mRNA transcript was used to assess the fold changes in KSHV ORF57, ORF47 and ORF65 between compound and DMSO treated reactivated (+DOX) TREx-BCBL-1-RTA cells by the $\Delta\Delta C_T$ method. **(D)** Reactivated TREx-BCBL-1-RTA cells were treated with 50 μM of MMV1645152 or compound 1 or compound 4 for 24 h qPCR analysis of KSHV ORF45 mRNA transcripts normalized to host GAPDH mRNA transcript was used to assess the fold changes in KSHV ORF45 between compound and DMSO treated reactivated (+DOX) TREx-BCBL-1-RTA cells by the $\Delta\Delta C_T$ method. **(E)–(I)** Reactivated TREx-BCBL-1-RTA cells were treated with 50 μM of MMV1645152 or compound 1 for 24 h (for ORFK8 and ORF50 analysis) or 48 h (for ORF10, ORF52 and ORF62 analyses). qPCR analysis of KSHV ORFK8, ORF10, ORF52, ORF62, and ORF50 mRNA transcripts normalized to host GAPDH mRNA transcript was used to assess the fold changes in KSHV ORFK8, ORF10, ORF52, ORF62, and ORF50 between compound and DMSO treated reactivated (+DOX) TREx-BCBL-1-RTA cells by the $\Delta\Delta C_T$ method. Statistical analysis comparing each treatment concentration to the reactivated DMSO control was determined by one-way ANOVA with Dunnett's multiple comparisons test where $^{*}P < 0.05$, $^{**}P < 0.01$, $^{***}P < 0.001$, and $^{****}P < 0.0001$ were considered significant.

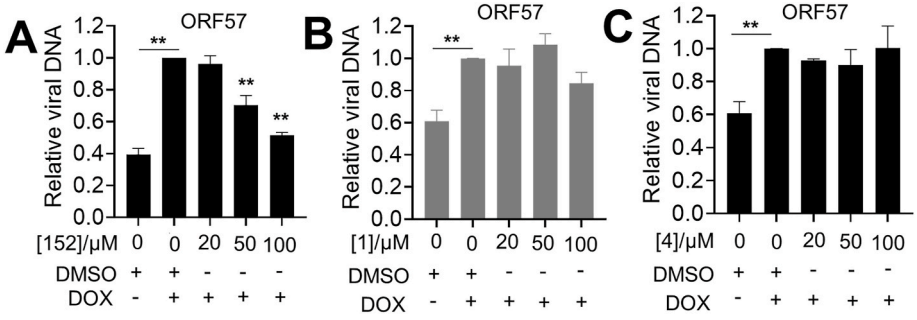

Fig. 5. MMV1645152 is more effective at inhibiting KSHV DNA replication than the selected structural analogues of MMV1645152. Reactivated TREx-BCBL-1-RTA cells were treated with increasing concentrations (0–100 μM) of **(A)** MMV1645152 or **(B)** compound 1 or **(C)** compound 4 for 72 h qPCR analysis of the viral genomic KSHV ORF57 gene normalized to the host genomic GAPDH gene was used to determine the fold change between compound and DMSO treated reactivated (+DOX) TREx-BCBL-1-RTA cells using the $\Delta\Delta C_T$ method. Unreactivated TREx-BCBL-1-RTA responses are indicated by -DOX. Statistical analysis comparing each treatment concentration to the reactivated DMSO control was determined by one-way ANOVA with Dunnett's multiple comparisons test where $^{**}P < 0.01$ was considered significant.

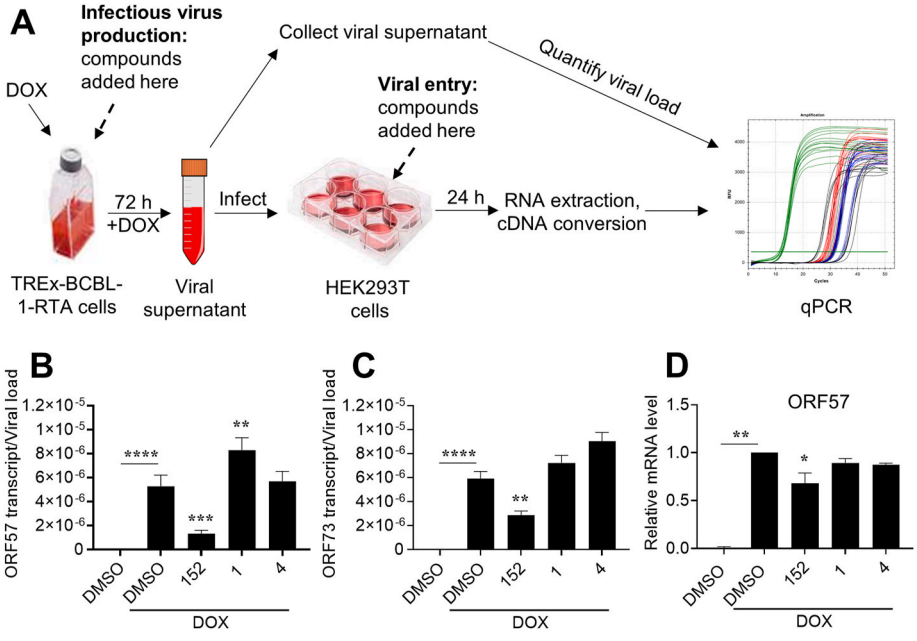

Fig. 6. MMV1645152 inhibits the production of infectious KSHV but not KSHV entry. (A) Workflow for re-infection assay to determine the production of infectious virion particles with treatment on TREx-BCBL-1-RTA cells or with treatment on HEK293T cells. **(B) and (C)** Reactivated TREx-BCBL-1-RTA cells were treated with either 50 μM MMV1645152 or compound 1 or compound 4 for 72 h. The viral supernatant was split into two parts – to infect HEK293T cells for 24 h and to determine viral load using qPCR analysis. KSHV ORF57 and KSHV ORF73 mRNA transcripts normalized to host GAPDH mRNA transcript in HEK293T cells were normalized to viral DNA load in each supernatant sample and was used to assess the level of KSHV infection in HEK293T cells. **(D)** TREx-BCBL-1-RTA cells were reactivated for 72 h. The viral supernatant was supplemented with either 50 μM MMV1645152 or compound 1 or compound 4 and used to infect HEK293T cells for 24 h qPCR analysis of KSHV ORF57 mRNA transcripts normalized to host GAPDH mRNA transcript was used to assess the level of KSHV infection in HEK293T cells. The $\Delta\Delta C_T$ method was used to determine the fold change in KSHV ORF57 mRNA transcript levels between the treated HEK293T cells and the untreated DMSO control. Statistical analysis comparing each treatment concentration to the reactivated DMSO control was determined by one-way ANOVA with Dunnett's multiple comparisons test where $^{**}P < 0.01$, $^{***}P < 0.001$, and $^{****}P < 0.0001$ were considered significant.

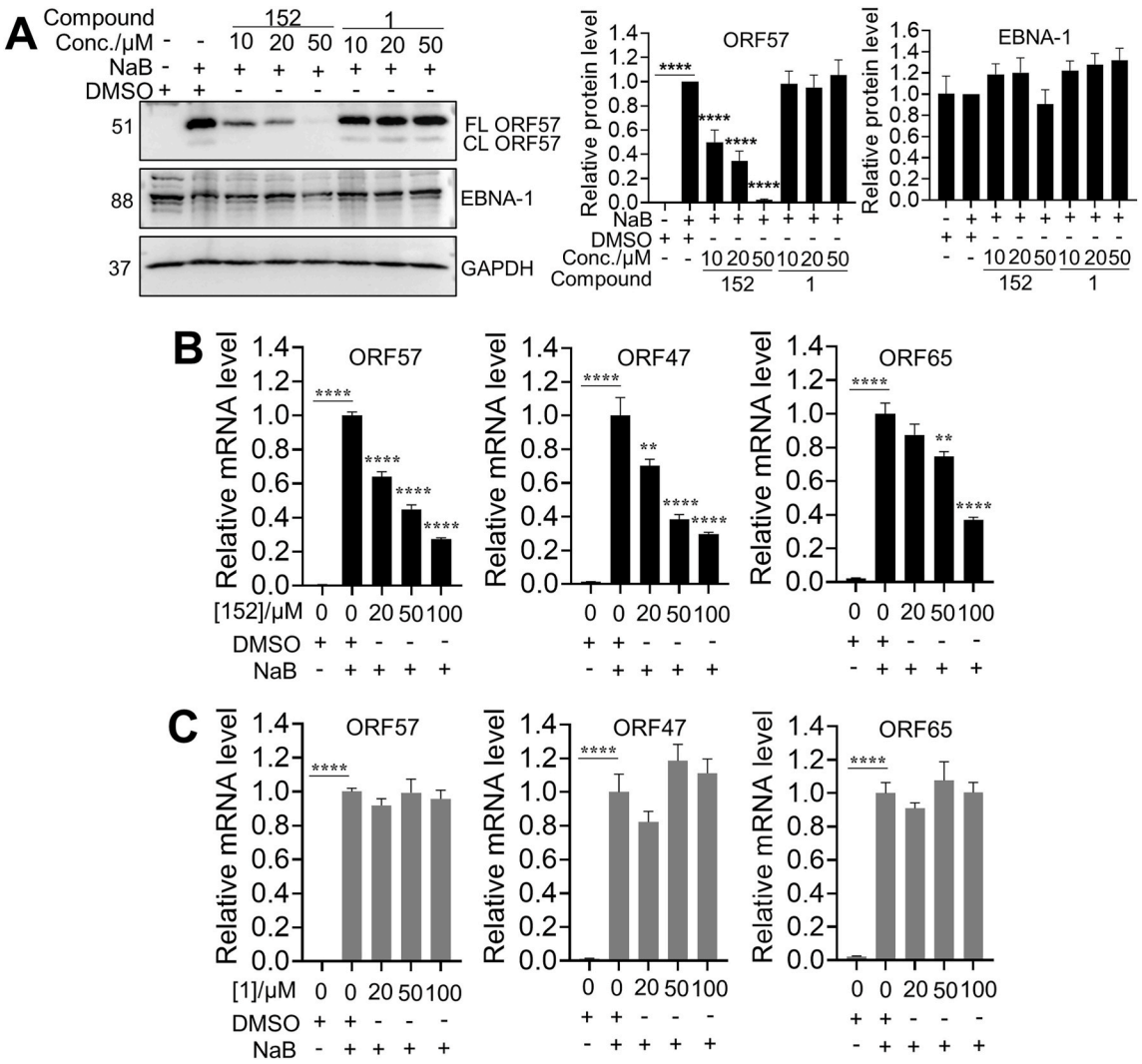

Fig. 7. MMV1645152 inhibits KSHV activity in reactivated BC-1 cells. (A) Western blot analysis and corresponding densitometry (using Image J) of KSHV ORF57 and EBV EBNA-1 protein levels relative to GAPDH in reactivated BC-1 cells treated with increasing concentrations (0–50 μM) of MMV1645152 or compound 1 for 24 h. The normalized expression of the target proteins in each sample was relativized to the reactivated DMSO control. **(B)** and **(C)** Reactivated BC-1 cells were treated with increasing concentrations (0–100 μM) of MMV1645152 or compound 1 for 24 h (for ORF57 analysis) or 48 h (for ORF47 and ORF65 analyses). qPCR analysis of KSHV ORF57, ORF47 and ORF65 mRNA transcripts normalized to host GAPDH mRNA transcript was used to assess the fold changes in gene expression levels of KSHV ORF57, ORF47, and ORF65 between compound and DMSO treated reactivated BC-1 cells by the $\Delta\Delta C_T$ method. Statistical analysis comparing each treatment concentration to the reactivated DMSO control was determined by one-way ANOVA with Dunnett's multiple comparisons test where $^{**}P < 0.01$ and $^{****}P < 0.0001$ were considered significant.

analysis. MMV1645152 significantly reduced the expression of KSHV ORF57 protein in a dose-dependent manner. However, compound 1 did not alter the expression of KSHV ORF57 protein (Fig. 8A).

Next, the gene expression of immediate early lytic genes (KSHV ORF57, ORF45, and ORF50), delayed early lytic gene (KSHV ORF47) and late lytic genes (KSHV ORF10, ORF52, and ORF65) in reactivated rKSHV.219 cells treated with 25 μM MMV1645152 or inactive analogue control compound 1 was evaluated. MMV1645152, but not compound 1, significantly reduced the gene expression levels of KSHV ORF57, ORF45, ORF47, ORF10, and ORF52 (Fig. 8B). However, MMV1645152 and compound 1 did not alter the expression level of KSHV ORF65 (Fig. 8B). This confirmed that MMV1645152, but not compound 1, specifically inhibited KSHV lytic gene expression. Furthermore, neither MMV1645152 nor compound 1 altered the expression level of KSHV ORF50 (Fig. 8B). This suggested that the anti-KSHV activity of MMV1645152 is not because of differential reactivation of rKSHV.219 cells. Taken together, these data confirm that MMV1645152 can target KSHV lytic replication in a range of cell types, including PEL and epithelial cell line models.

4. Discussion

KSHV lytic replication plays a key role in the onset of KSHV infection and tumorigenesis, and therefore inhibiting KSHV lytic replication is a promising strategy for KSHV therapy. In this study, the protein level of KSHV ORF57 was used to monitor KSHV reactivation and lytic replication in TREx-BCBL-1-RTA cells. Using KSHV ORF57 levels as the primary screen, we report the identification of a novel KSHV inhibitor from the MMV Pandemic Response Box. MMV1645152 reduced lytic gene and protein expression, reduced KSHV viral DNA replication and inhibited production of infectious virions. Also, the inhibition of KSHV lytic gene expression and KSHV ORF57 protein was replicated in the context of EBV infection and in a KS epithelial cell line model. To the best of our knowledge, this is the first study to use KSHV ORF57 protein level as a marker to screen drug-like compounds for inhibitors of KSHV reactivation and lytic replication and demonstrates that anti-KSHV

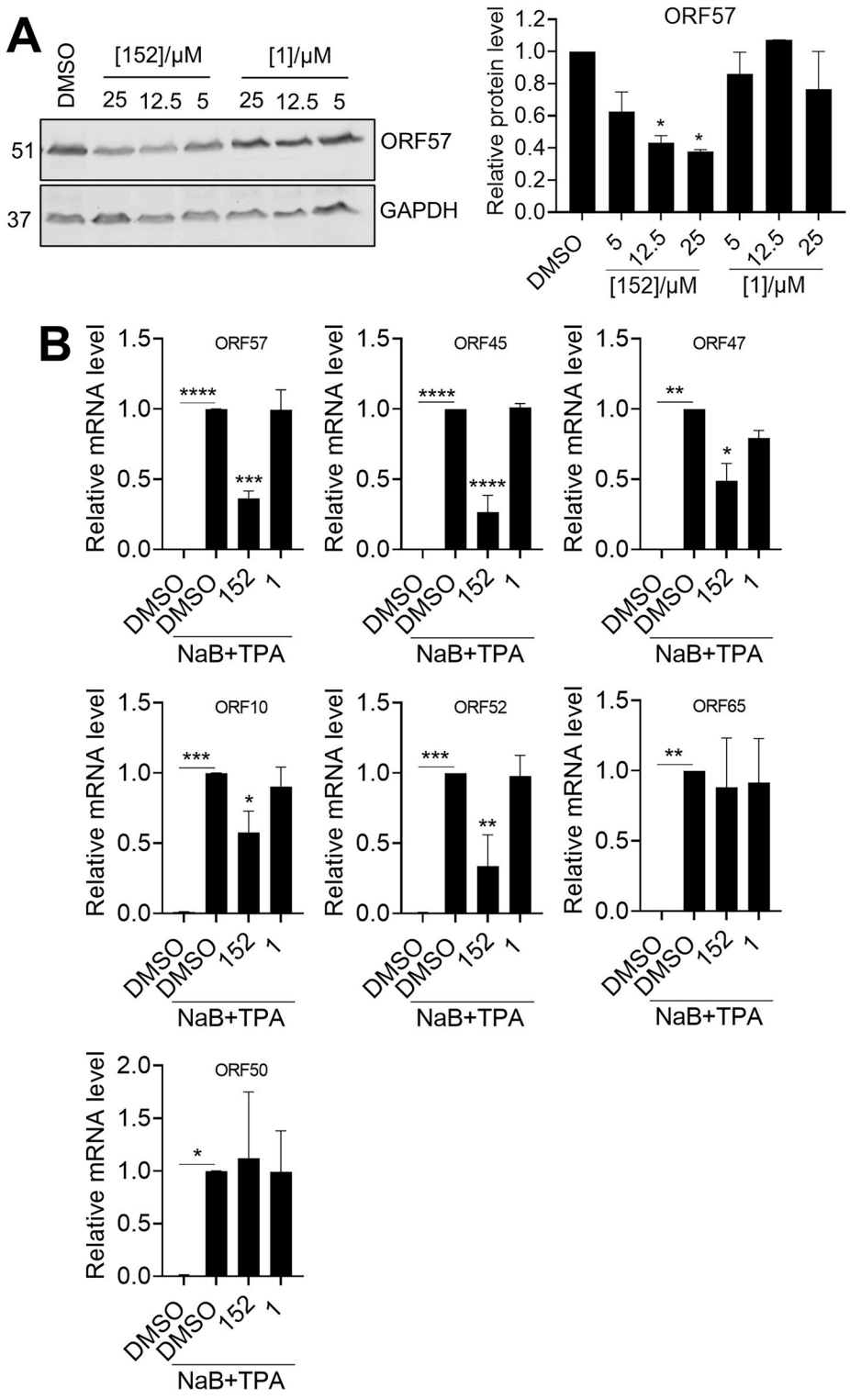

Fig. 8. MMV1645152 inhibits KSHV activity in reactivated rKSHV.219 cells. (A) Western blot analysis and corresponding densitometry (using Image J) of KSHV ORF57 protein levels relative to GAPDH in reactivated rKSHV.219 cells treated with increasing concentrations (0–25 μM) of MMV1645152 or compound 1 for 24 h. The normalized expression of KSHV ORF57 protein in each sample was relativized to the reactivated DMSO control. **(B)** and **(C)** Reactivated rKSHV.219 cells were treated with 25 μM MMV1645152 or compound 1 for 24 h qPCR analysis of KSHV ORF57, ORF45, ORF47, ORF10, ORF52, ORF65, and ORF50 mRNA transcripts normalized to host GAPDH mRNA transcript was used to assess the fold changes in gene expression levels of KSHV ORF57, ORF45, ORF47, ORF10, ORF52, ORF65, and ORF50 between compound and DMSO treated reactivated rKSHV.219 cells by the $\Delta\Delta C_T$ method. Statistical analysis comparing each treatment concentration to the reactivated DMSO control was determined by one-way ANOVA with Dunnett's multiple comparisons test where $^{*}P < 0.05$, $^{**}P < 0.01$, $^{***}P < 0.001$, and $^{****}P < 0.0001$ were considered significant.

compounds with novel modes of action can be identified from existing libraries. This is the first study to report that MMV1645152 (2-amino-5-bromo-6-(3-chlorophenyl)-1H-pyrimidin-4-one) is an inhibitor of KSHV lytic replication.

Of the 153 antiviral compounds contained in MMV Pandemic Response Box, 10 (to the best of our knowledge) have been reported in the literature as potential therapeutic agents against herpesvirus infections. Based on the selection criteria set for the initial screening of the MMV Pandemic Response Box at 20 μM, MMV1645152 was a more potent inhibitor of KSHV lytic replication. These compounds include MMV1593517 (selinexor), which showed some activity against KSHV (Meng and Gao, 2021); MMV690653 (letermovir) against CMV (Asha and Sharma-Walia, 2021; Cassaniti et al., 2021); MMV1580478 (tenofovir) against KSHV (Tian et al., 2008); MMV009948 (imatinib), which has passed phase II trial, and is active against KSHV (Campione et al., 2009; Cao et al., 2015; Koon et al., 2014); MMV639951 (everolimus) against KSHV (Mohanty et al., 2017); MMV001761 (ganciclovir) against KSHV (Casper et al., 2004; Chatterjee et al., 2012; Gantt et al., 2011; Parsons et al., 2006); MMV001961 (acyclovir) against KSHV (Kedes and Ganem, 1997); MMV1580493 (verdinexor) against KSHV (Widman et al., 2018); MMV1580486 (pritelivir) against HSV-1 and -2 (Quenelle et al., 2018); and MMV1782210 (cyclopropavir) against HCMV, HHV6A, HHV6B, and KSHV (James et al., 2011; Manners et al., 2018). The initial phenotype-based screening was performed blind without prior knowledge of the antiviral activity of the compounds in the Pandemic Response Box and none of the above-mentioned compounds were identified in our screen. This is likely due to the criteria of the screen which was focused on inhibitors of KSHV lytic replication using the early gene ORF57 as a marker, while most of the above-mentioned antiviral compounds (example acyclovir, tenofovir, pritelivir, and ganciclovir) target other processes like DNA replication which occur later in the lifecycle of KSHV. A good antiviral drug should ideally reduce viral DNA or infectivity by a thousand-fold at sub-micromolar concentrations. However, the low micromolar IC_{50} for ORF57 inhibition and the novel mechanism of action were deemed sufficient to prioritize MMV1645152.

The four structural analogues used in this study to investigate the specificity of MMV1645152's anti-KSHV activities all belong to the pyrimidinone group of chemical compounds but differ from MMV1645152 in the number or position of halogen atom(s) (Figs. 2A and 3B), which appear critical for the anti-KSHV activity of MMV1645152. Like MMV1645152, compound 4 has a bromine atom in position number 5 and significantly reduced KSHV ORF57 protein level (Fig. 3C–D). However, none of the structural analogues had a chlorine atom in position number 3 of the phenyl side chain, and this may explain the difference in biological activity between MMV1645152 and the structural analogues.

Our results also indicate that MMV1645152 has a novel mode of anti-KSHV action that remains to be defined. MMV1645152 (2-amino-5-bromo-6-(3-chlorophenyl)-1H-pyrimidin-4-one) is a member of the pyrimidinone group of compounds previously shown to induce interferon production as an antiviral response (Skulnick et al., 1985; Stringfellow, 1981; Wierenga, 1985; Wierenga et al., 1980). Analogue 4, which was partially active in our assays, is bropirimine (PNU-54461/ABPP), an experimental anti-cancer agent evaluated for treatment of viral infections, autoimmune disorders and bladder cancer (Akaza et al., 1998; A. H et al., 1997; F. H et al., 1997; Sarosdy et al., 2005; Sidwell et al., 1994; Suzuki et al., 2015; Vroegop et al., 1999; Witjes et al., 1999). Bropirimine is an agonist of Toll-like receptor 7 (TLR7) leading to activation of TLR7 signaling and the production of cytokines including interferon α/β (Akira and Hemmi, 2003; Suzuki et al., 2015; Vroegop et al., 1999). TLR signaling is implicated in reactivation of KSHV from latency (Gregory et al., 2009), and both TLR7 and interferons are central to the KSHV antiviral response and are modulated by viral mimics of host interferon regulatory factors (vIRF1-4) (Jacobs and Damania, 2011; Sathish and Yuan, 2011). Interferon α is sufficient to reduce KSHV DNA load and viral gene expression (Monini et al., 1999), including via increases in IFIT levels which reduce lytic replication (Li and Swaminathan, 2019). Therefore, it is plausible that the production of interferon α/β by bropirimine (compound 4) explains the partial reduction in KSHV lytic replication. We speculate that, based on the structural similarity, the increased activity of MMV1645152 was due to a similar mechanism of action. If correct, then the increased anti-KSHV activity of MMV1645152 should induce higher levels of interferon α/β production. Unexpectedly however, preliminary data from our group suggest that MMV1645152 treatment in fact reduced interferon α production during KSHV lytic replication (data not shown). This suggests that the chemical modifications to bropirimine to produce in MMV1645152 reduce interferon production and result in an alternative mechanism of action. The reduction in KSHV lytic replication induced by MMV1645152 may translate into a concomitant reduction in interferon production (Tabtieng et al., 2018; Zhang et al., 2020). However, further investigation into the mechanism of action of MMV1645152 is needed to draw a mechanistic conclusion. Therefore, additional experiments to understand the anti-KSHV mechanism of MMV1645152 in detail and to generate more potent analogues are ongoing.

Funding

This research was funded by an Academy of Medical Sciences Newton Advanced Fellowship and Department of Science and Innovation and National Research Foundation, DSI/NRF) South African Research Chair (SARChI) grant (Grant number: 98566). This project was also funded by the MRC Africa Research Leaders award (MR/V030701/1) which is jointly funded by the UK Medical Research Council (MRC) and the UK Foreign, Commonwealth & Development Office (FCDO) under the MRC/FCDO Concordat agreement and is carried out in the frame of the Global Health EDCTP3 Joint Undertaking. CGLV gratefully acknowledges support from Future Leaders – African Independent Research (FLAIR), a partnership between the African Academy of Sciences and the Royal Society that is funded by the UK Government as part of the Global Challenge Research Fund (GCRF). MMV provided funding in kind through donation of the Pandemic Response Box.

CRediT authorship contribution statement

Michael O. Okpara: Writing – original draft, Methodology, Investigation, Formal analysis, Data curation, Conceptualization. **Frederick Weaver:** Formal analysis, Investigation, Methodology, Writing – review & editing. **Adrian Whitehouse:** Writing – review & editing, Methodology, Funding acquisition, Formal analysis, Conceptualization. **Clinton G.L. Veale:** Writing – review & editing, Resources, Funding acquisition, Formal analysis. **Adrienne L. Edkins:** Writing – review & editing, Supervision, Resources, Project administration, Methodology, Funding acquisition, Data curation, Conceptualization.

Declaration of competing interest

The authors declare that they have no known competing financial interests or personal relationships that could have appeared to influence the work reported in this paper.

Data availability

Data will be made available on request.

Acknowledgements

We thank the Medicines for Malaria Venture (MMV) for providing the Pandemic Response Box.

Appendix A. Supplementary data

Supplementary data to this article can be found online at https://doi.org/10.1016/j.antiviral.2024.105990.

References

Akaza, H., Kotake, T., Machida, T., 1998. Bropirimine, an orally active anticancer agent for superficial bladder cancer. Eur. Urol. 34, 107–110. https://doi.org/10.1159/000019693.

Akira, S., Hemmi, H., 2003. Recognition of pathogen-associated molecular patterns by TLR family. Immunol. Lett. 85, 85–95. https://doi.org/10.1016/S0165-2478(02)00228-6.

Andrei, G., Snoeck, R., 2015. Kaposi's sarcoma-associated herpesvirus: the role of lytic replication in targeted therapy. Curr. Opin. Infect. Dis. 28, 611–624. https://doi.org/10.1097/QCO.0000000000000213.

Aneja, K.K., Yuan, Y., 2017. Reactivation and lytic replication of Kaposi's sarcoma-associated herpesvirus: an update. Front. Microbiol. 8, 1–23. https://doi.org/10.3389/fmicb.2017.00613.

Asha, K., Sharma-Walia, N., 2021. Targeting host cellular factors as a strategy of therapeutic intervention for herpesvirus infections. Front. Cell. Infect. Microbiol. 11, 1–19. https://doi.org/10.3389/fcimb.2021.603309.

Bounaadja, L., Piret, J., Goyette, N., Boivin, G., 2013. Evaluation of epstein-barr virus, human herpesvirus 6 (HHV-6), and HHV-8 antiviral drug susceptibilities by use of real-time-pcrbased assays. J. Clin. Microbiol. 51, 1244–1246. https://doi.org/10.1128/JCM.03234-12.

Bouvard, V., Baan, R., Straif, K., Grosse, Y., Secretan, B., El Ghissassi, F., Benbrahim-Tallaa, L., Guha, N., Freeman, C., Galichet, L., Cogliano, V., 2009. A review of human carcinogens–Part B: biological agents. Lancet Oncol. 10, 321–322. https://doi.org/10.1016/s1470-2045(09)70096-8.

Boyne, J.R., Colgan, K.J., Whitehouse, A., 2008. Recruitment of the complete hTREX complex is required for Kaposi's sarcoma-associated herpesvirus intronless mRNA nuclear export and virus replication. PLoS Pathog. 4, 1–16. https://doi.org/10.1371/journal.ppat.1000194.

Boyne, J.R., Jackson, B.R., Taylor, A., MacNab, S.A., Whitehouse, A., 2010. Kaposi's sarcoma-associated herpesvirus ORF57 protein interacts with PYM to enhance translation of viral intronless mRNAs. EMBO J. 29, 1851–1864. https://doi.org/10.1038/emboj.2010.77.

Bustin, S.A., Benes, V., Garson, J.A., Hellemans, J., Huggett, J., Kubista, M., Mueller, R., Nolan, T., Pfaffl, M.W., Shipley, G.L., Vandesompele, J., Wittwer, C.T., 2009. The MIQE guidelines: minimum information for publication of quantitative real-time PCR experiments. Clin. Chem. 55, 611–622. https://doi.org/10.1373/clinchem.2008.112797.

Campione, E., Diluvio, L., Paternò, E.J., Di Marcantonio, D., Francesconi, A., Terrinoni, A., Orlandi, A., Chimenti, S., 2009. Kaposi's sarcoma in a patient treated with imatinib mesylate for chronic myeloid leukemia. Clin. Therapeut. 31, 2565–2569. https://doi.org/10.1016/j.clinthera.2009.11.018.

Cao, W., Vyboh, K., Routy, B., Chababi-Atallah, M., Lemire, B., Routy, J.P., 2015. Imatinib for highly chemoresistant Kaposi sarcoma in a patient with long-term HIV control: a case report and literature review. Curr. Oncol. 22, e395–e399. https://doi.org/10.3747/co.22.2635.

Casper, C., Nichols, W.G., Huang, M.L., Corey, L., Wald, A., 2004. Remission of HHV-8 and HIV-associated multicentric Castleman disease with ganciclovir treatment. Blood 103, 1632–1634. https://doi.org/10.1182/blood-2003-05-1721.

Cassaniti, I., Colombo, A.A., Bernasconi, P., Malagola, M., Russo, D., Iori, A.P., Girmenia, C., Greco, R., Peccatori, J., Ciceri, F., Bonifazi, F., Percivalle, E., Campanini, G., Piccirilli, G., Lazzarotto, T., Baldanti, F., 2021. Positive HCMV DNAemia in stem cell recipients undergoing letermovir prophylaxis is expression of abortive infection. Am. J. Transplant. 21, 1622–1628. https://doi.org/10.1111/ajt.16450.

Cesarman, E., Chadburn, A., Rubinstein, P.G., 2022. KSHV/HHV8-mediated hematologic diseases. Blood 139, 1013–1025. https://doi.org/10.1182/blood.2020005470.

Chatterjee, D., Chandran, B., Berger, E.A., 2012. Selective killing of Kaposi's sarcoma-associated herpesvirus lytically infected cells with a recombinant immunotoxin targeting the viral gpK8.1A envelope glycoprotein. mAbs 4, 233–242. https://doi.org/10.4161/mabs.4.2.19262.

Chen, C.J., You, S.L., Hsu, W.L., Yang, H.I., Lee, M.H., Chen, H.C., Chen, Y.Y., Liu, J., Hu, H.H., Lin, Y.J., Chu, Y.J., Huang, Y.T., Chiang, C.J., Chien, Y.C., 2021. Epidemiology of virus infection and human cancer. Recent Results Cancer Res. 217, 13–45. https://doi.org/10.1007/978-3-030-57362-1_2.

Coen, N., Duraffour, S., Snoeck, R., Andrei, G., 2014. KSHV targeted therapy: an update on inhibitors of viral lytic replication. Viruses 6, 4731–4759. https://doi.org/10.3390/v6114731.

Gantt, S., Carlsson, J., Ikoma, M., Gachelet, E., Gray, M., Geballe, A.P., Corey, L., Casper, C., Lagunoff, M., Vieira, J., 2011. The HIV protease inhibitor nelfinavir inhibits Kaposi's sarcoma-associated herpesvirus replication in vitro. Antimicrob. Agents Chemother. 55, 2696–2703. https://doi.org/10.1128/AAC.01295-10.

Goodwin, D.J., Walters, M.S., Smith, P.G., Thurau, M., Fickenscher, H., Whitehouse, A., 2001. Herpesvirus Saimiri open reading frame 50 (rta) protein reactivates the lytic replication cycle in a persistently infected A549 cell line. J. Virol. 75, 4008–4013. https://doi.org/10.1128/jvi.75.8.4008-4013.2001.

Gould, F., Harrison, S.M., Hewitt, E.W., Whitehouse, A., 2009. Kaposi's sarcoma-associated herpesvirus RTA promotes degradation of the Hey1 repressor protein through the ubiquitin proteasome pathway. J. Virol. 83, 6727–6738. https://doi.org/10.1128/jvi.00351-09.

Graham, F.L., Smiley, J., Russell, W.C., Nairn, R., 1977. Characteristics of a human cell line transformed by DNA from human adenovirus type 5. J. Gen. Virol. 36, 59–72. https://doi.org/10.1099/0022-1317-36-1-59.

Gregory, S.M., West, J.A., Dillon, P.J., Hilscher, C., Dittmer, D.P., Damania, B., 2009. Toll-like receptor signaling controls reactivation of KSHV from latency. Proc. Natl. Acad. Sci. U.S.A. 106, 11725–11730. https://doi.org/10.1073/pnas.0905316106.

H, A., J, S., K, T., T, K., E, O., S, K.T.M., 1997. [Bropirimine (U-54461S) Late Phase II Clinical Study for Carcinoma in Situ of the Bladder. Japan Bropirimine Study Group], vol. 24. Gan To Kagaku Ryoho, pp. 77–85.

Han, Z., Swaminathan, S., 2006. Kaposi's sarcoma-associated herpesvirus lytic gene ORF57 is essential for infectious virion production. J. Virol. 80, 5251–5260. https://doi.org/10.1128/jvi.02570-05.

Jacobs, S.R., Damania, B., 2011. The viral interferon regulatory factors of KSHV: immunosuppressors or oncogenes? Front. Immunol. 2, 1–11. https://doi.org/10.3389/fimmu.2011.00019.

James, S.H., Hartline, C.B., Harden, E.A., Driebe, E.M., Schupp, J.M., Engelthaler, D.M., Keim, P.S., Bowlin, T.L., Kern, E.R., Prichard, M.N., 2011. Cyclopropavir inhibits the normal function of the human cytomegalovirus UL97 kinase. Antimicrob. Agents Chemother. 55, 4682–4691. https://doi.org/10.1128/AAC.00571-11.

Kedes, D.H., Ganem, D., 1997. Sensitivity of Kaposi's sarcoma-associated herpesvirus replication to antiviral drugs: implications for potential therapy. J. Clin. Invest. 99, 2082–2086. https://doi.org/10.1172/JCI119380.

Kirigin, E., Ruck, D.K., Jackson, Z., Murphy, J., McDonnell, E., Okpara, M.O., Whitehouse, A., Edkins, A.L., 2020. Regulation of Kaposi's sarcoma-associated herpesvirus biology by host molecular chaperones. In: Heat Shock Proteins. Springer, Dordrecht, Dordrecht. https://doi.org/10.1007/7515_2020_18.

Koon, H.B., Krown, S.E., Lee, J.Y., Honda, K., Rapisuwon, S., Wang, Z., Aboulafia, D., Reid, E.G., Rudek, M.A., Dezube, B.J., Noy, A., 2014. Phase II trial of imatinib in AIDS-associated Kaposi's sarcoma: AIDS malignancy consortium protocol 042. J. Clin. Oncol. 32, 402–408. https://doi.org/10.1200/JCO.2012.48.6365.

Li, D., Swaminathan, S., 2019. Human IFIT proteins inhibit lytic replication of KSHV: a new feed-forward loop in the innate immune system. PLoS Pathog. 15, 1–27. https://doi.org/10.1371/journal.ppat.1007609.

Lunn, R.M., Jahnke, G.D., Rabkin, C.S., 2017. Tumour virus epidemiology. Philos. Trans. R. Soc. B Biol. Sci. 372 https://doi.org/10.1098/rstb.2016.0266.

Majerciak, V., Zheng, Z.M., 2009. Kaposi's sarcoma-associated herpesvirus ORF57 in viral RNA processing. Front. Biosci. 14, 1516–1528. https://doi.org/10.2741/3322.

Manners, O., Murphy, J.C., Coleman, A., Hughes, D.J., Whitehouse, A., 2018. Contribution of the KSHV and EBV lytic cycles to tumourigenesis. Curr. Opin. Virol. 32, 60–70. https://doi.org/10.1016/j.coviro.2018.08.014.

Medicines for Malaria Venture, 2019. About the pandemic response box [WWW Document]. URL. https://www.mmv.org/mmv-open/pandemic-response-box/about-pandemic-response-box. (Accessed 4 April 2020).

Meng, W., Gao, S.J., 2021. Targeting XPO1 enhances innate immune response and inhibits KSHV lytic replication during primary infection by nuclear stabilization of the p62 autophagy adaptor protein. Cell Death Dis. 12, 1–16. https://doi.org/10.1038/s41419-020-03303-1.

Mohanty, S., Kumar, A., Das, P., Sahu, S.K., Choudhuri, T., 2017. Multi-targeted therapy of everolimus in Kaposi's sarcoma associated herpes virus infected primary effusion lymphoma. Apoptosis 22, 1098–1115. https://doi.org/10.1007/s10495-017-1391-1.

Monini, P., Carlini, F., Stürzl, M., Rimessi, P., Superti, F., Franco, M., Melucci-Vigo, G., Cafaro, A., Goletti, D., Sgadari, C., Butto, S., Leone, Patrizia, Leone, Pasqualina, Chiozzini, C., Barresi, C., Tinari, A., Bonaccorsi, A., Capobianchi, M.R., Giuliani, M., di Carlo, A., Andreoni, M., Rezza, G., Ensoli, B., 1999. Alpha interferon inhibits human herpesvirus 8 (HHV-8) reactivation in primary effusion lymphoma cells and reduces HHV-8 load in cultured peripheral blood mononuclear cells. J. Virol. 73, 4029–4041. https://doi.org/10.1128/jvi.73.5.4029-4041.1999.

Murphy, J.C., Harrington, E.M., Schumann, S., Vasconcelos, E.J.R., Mottram, T.J., Harper, K.L., Aspden, J.L., Whitehouse, A., 2023. Kaposi's sarcoma-associated herpesvirus induces specialised ribosomes to efficiently translate viral lytic mRNAs. Nat. Commun. 14 https://doi.org/10.1038/s41467-023-35914-5.

Naimo, E., Zischke, J., Schulz, T.F., 2021. Recent advances in developing treatments of Kaposi's sarcoma herpesvirus-related diseases. Viruses 13, 1–16. https://doi.org/10.3390/v13091797Academic.

Nakamura, H., Lu, M., Gwack, Y., Souvlis, J., Zeichner, S.L., Jung, J.U., 2003. Global changes in Kaposi's sarcoma-associated virus gene expression patterns following expression of a tetracycline-inducible rta transactivator. J. Virol. 77, 4205–4220. https://doi.org/10.1128/jvi.77.7.4205-4220.2003.

Nichols, L.A., Adang, L.A., Kedes, D.H., 2011. Rapamycin blocks production of KSHV/HHV8: insights into the anti-tumor activity of an immunosuppressant drug. PLoS One 6. https://doi.org/10.1371/journal.pone.0014535.

Ozbalak, M., Tokatli, I., Özdemirli, M., Tecimer, T., Ar, M.C., Örnek, S., Koroglu, A., Laleli, Y., Ferhanoglu, B., 2013. Is valganciclovir really effective in primary effusion lymphoma: case report of an HIV(-) EBV(-) HHV8(+) patient. Eur. J. Haematol. 91, 467–469. https://doi.org/10.1111/ejh.12174.

Parsons, C.H., Adang, L.A., Overdevest, J., O'Connor, C.M., Taylor, J.R., Camerini, D., Kedes, D.H., 2006. KSHV targets multiple leukocyte lineages during long-term productive infection in NOD/SCID mice. J. Clin. Invest. 116, 1963–1973. https://doi.org/10.1172/JCI27249.

Purushothaman, P., Uppal, T., Verma, S.C., 2015. Molecular biology of KSHV lytic reactivation. Viruses 7, 116–153. https://doi.org/10.3390/v7010116.

Quenelle, D.C., Birkmann, A., Goldner, T., Pfaff, T., Zimmermann, H., Bonsmann, S., Collins, D.J., Rice, T.L., Prichard, M.N., 2018. Efficacy of pritelivir and acyclovir in the treatment of herpes simplex virus infections in a mouse model of herpes simplex

encephalitis. Antivir. Res. 149, 1–6. https://doi.org/10.1016/j.antiviral.2017.11.002.
Samby, K., Besson, D., Dutta, A., Patra, B., Doy, A., Glossop, P., Mills, J., Whitlock, G., Hooft Van Huijsduijnen, R., Monaco, A., Bilbe, G., Mowbray, C., Perry, B., Adam, A., Wells, T.N.C., Willis, P.A., 2022. The pandemic response box-accelerating drug discovery efforts after disease outbreaks. ACS Infect. Dis. 8, 713–720. https://doi.org/10.1021/acsinfecdis.1c00527.
Sandhu, P.K., Damania, B., 2022. The regulation of KSHV lytic reactivation by viral and cellular factors. Curr. Opin. Virol. 52, 39–47. https://doi.org/10.1016/j.coviro.2021.11.004.
Sarosdy, M.F., Tangen, C.M., Weiss, G.R., Nestok, B.R., Benson, M.C., Schellhammer, P. F., Sagalowsky, A.I., Wood, D.P., Crawford, E.D., 2005. A phase II clinical trial of oral bropirimine in combination with intravesical bacillus Calmette-Guérin for carcinoma in situ of the bladder: a Southwest Oncology Group Study. Urol. Oncol. Semin. Orig. Investig. 23, 386–389. https://doi.org/10.1016/j.urolonc.2005.05.028.
Sathish, N., Yuan, Y., 2011. Evasion and subversion of interferon-mediated antiviral immunity by Kaposi's sarcoma-associated herpesvirus: an overview. J. Virol. 85, 10934–10944. https://doi.org/10.1128/jvi.00687-11.
Schmittgen, T.D., Livak, K.J., 2008. Analyzing real-time PCR data by the comparative CT method. Nat. Protoc. 3, 1101–1108. https://doi.org/10.1038/nprot.2008.73.
Schumann, S., Jackson, B.R., Yule, I., Whitehead, S.K., Revill, C., Foster, R., Whitehouse, A., 2016. Targeting the ATP-dependent formation of herpesvirus ribonucleoprotein particle assembly as an antiviral approach. Nat. Microbiol. 2 https://doi.org/10.1038/nmicrobiol.2016.201.
Sidwell, R.W., Huffman, J.H., Barnard, D.L., Smee, D.F., Warren, R.P., Chirigos, M.A., Kende, M., Huggins, J., 1994. Antiviral and immunomodulating inhibitors of experimentally-induced Punta Toro virus infections. Antivir. Res. 25, 105–122. https://doi.org/10.1016/0166-3542(94)90100-7.
Skulnick, H.I., Weed, S.D., Eidson, E.E., Renis, H.E., Wierenga, W., Stringfellow, D.A., 1985. Pyrimidinones. 1. 2-Amino-5-halo-6-aryl-4(3H)-pyrimidinones. Interferon-inducing antiviral agents. J. Med. Chem. 28, 1864–1869. https://doi.org/10.1021/jm00150a018.
Smith, P.K., Krohn, R.I., Hermanson, G.T., Mallia, A.K., Gartner, F.H., Provenzano, M.D., Fujimoto, E.K., Goeke, N.M., Olson, B.J., Klenk, D.C., 1985. Measurement of protein using bicinchoninic acid. Anal. Biochem. 150, 76–85. https://doi.org/10.1016/0003-2697(85)90442-7.
Stringfellow, D.A., 1981. Antineoplastic properties of pyrimidinone interferon inducers. Adv. Enzym. Regul. 19, 335–348. https://doi.org/10.1016/0065-2571(81)90023-6.
Suzuki, H., Mochizuki, A., Yoshimura, K., Miyamoto, Y., Kaneko, K., Inoue, T., Chikazu, D., Takami, M., Kamijo, R., 2015. Bropirimine inhibits osteoclast differentiation through production of interferon-β. Biochem. Biophys. Res. Commun. 467, 146–151. https://doi.org/10.1016/j.bbrc.2015.09.092.
Tabtieng, T., Degterev, A., Gaglia, M.M., 2018. Caspase-dependent suppression of type I interferon signaling promotes Kaposi's sarcoma-associated herpesvirus lytic replication. Virology 92, 1–17.
Tian, R.R., Liao, Q.J., Chen, X., 2008. Prevention and treatment of KSHV-associated diseases with antiviral drugs. Virol. Sin. 23, 486–495. https://doi.org/10.1007/s12250-008-2995-y.
Uldrick, T.S., Polizzotto, M.N., Aleman, K., O'Mahony, D., Wyvill, K.M., Wang, V., Marshall, V., Pittaluga, S., Steinberg, S.M., Tosato, G., Whitby, D., Little, R.F., Yarchoan, R., 2011. High-dose zidovudine plus valganciclovir for Kaposi sarcoma herpesvirus-associated multicentric Castleman disease: a pilot study of virus-activated cytotoxic therapy. Blood 117, 6977–6986. https://doi.org/10.1182/blood-2010-11-317610.
Uldrick, T.S., Polizzotto, M.N., Yarchoan, R., 2012. Recent advances in Kaposi sarcoma herpesvirus-associated multicentric Castleman disease. Curr. Opin. Oncol. 24, 495–505. https://doi.org/10.1097/CCO.0b013e328355e0f3.
Upadhyayula, S., Michaels, M.G., 2013. Ganciclovir, foscarnet, and cidofovir: antiviral drugs not just for Cytomegalovirus. J. Pediatric Infect. Dis. Soc. 2, 286–290. https://doi.org/10.1093/jpids/pit048.
Veale, C.G.L., 2019. Unpacking the pathogen box—an open source tool for fighting neglected tropical disease. ChemMedChem. https://doi.org/10.1002/cmdc.201800755.
Verma, D., Li, D.-J., Krueger, B., Renne, R., Swaminathan, S., 2015. Identification of the physiological gene targets of the essential lytic replicative Kaposi's sarcoma-associated herpesvirus ORF57 protein. J. Virol. 89, 1688–1702. https://doi.org/10.1128/jvi.02663-14.
Vieira, J., O'Hearn, P.M., 2004. Use of the red fluorescent protein as a marker of Kaposi's sarcoma-associated herpesvirus lytic gene expression. Virology 325, 225–240. https://doi.org/10.1016/j.virol.2004.03.049.
Vroegop, S.M., Chapman, D.L., Decker, D.E., Galinet, L.A., Brideau, R.J., Ready, K.A., Dunn, C.J., Buxser, S.E., 1999. Pharmacokinetic properties, induction of interferon, and efficacy of selected 5-halo-6-phenyl pyrimidinones, bropirimine analogues, in a model of severe experimental autoimmune encephalomyelitis. Int. J. Immunopharm. 21, 647–662. https://doi.org/10.1016/S0192-0561(99)00040-5.
Widman, D.G., Gornisiewicz, S., Shacham, S., Tamir, S., 2018. In vitro toxicity and efficacy of verdinexor, an exportin 1 inhibitor, on opportunistic viruses affecting immunocompromised individuals. PLoS One 13, 1–18. https://doi.org/10.1371/journal.pone.0200043.
Wierenga, W., 1985. Antiviral and other bioactivities of pyrimidinones. Pharmacol. Ther. 30, 67–89. https://doi.org/10.1016/0163-7258(85)90048-8.
Wierenga, W., Skulnick, H.I., Stringfellow, D.A., Weed, S.D., Renis, H.E., Eidson, E.E., 1980. 5-Substituted 2-Amino-6-phenyl-4(3H)-pyrimidinones. Antiviral- and interferon-inducing agents. J. Med. Chem. 23, 237–239. https://doi.org/10.1021/jm00177a004.
Witjes, W.P.J., Konig, M., Boeminghaus, F.P., Hall, R.R., Schulman, C.C., Zurlo, M., Fittipaldo, A., Riggi, M., Debruyne, F.M.J., 1999. Results of a European comparative randomized study comparing oral bropirimine versus intravesical BCG treatment in BCG-naive patients with carcinoma in situ of the urinary bladder. Eur. Urol. 36, 576–581. https://doi.org/10.1159/000020051.
Zhang, H., Ni, G., Damania, B., 2020. ADAR1 facilitates KSHV lytic reactivation by modulating the RLR-dependent signaling pathway. Cell Rep. 31, 1–13. https://doi.org/10.1016/j.celrep.2020.107564.